Biosafety Studies of a Clinically Applicable Lentiviral Vector for the Gene Therapy of Artemis-SCID

S. Charrier, C. Lagresle-Peyrou, V. Poletti, M. Rothe, G. Cedrone, B. Gjata, F. Mavilio, A. Fischer, A. Schambach, J. P. De Villartay, et al.

▶ **To cite this version:**

S. Charrier, C. Lagresle-Peyrou, V. Poletti, M. Rothe, G. Cedrone, et al.. Biosafety Studies of a Clinically Applicable Lentiviral Vector for the Gene Therapy of Artemis-SCID. Mol Ther Methods Clin Dev, 2019, 15, pp.232-245. 10.1016/j.omtm.2019.08.014 . hal-02880790

HAL Id: hal-02880790
https://hal.science/hal-02880790

Submitted on 20 Jul 2022

HAL is a multi-disciplinary open access archive for the deposit and dissemination of scientific research documents, whether they are published or not. The documents may come from teaching and research institutions in France or abroad, or from public or private research centers.

L'archive ouverte pluridisciplinaire **HAL**, est destinée au dépôt et à la diffusion de documents scientifiques de niveau recherche, publiés ou non, émanant des établissements d'enseignement et de recherche français ou étrangers, des laboratoires publics ou privés.

Distributed under a Creative Commons Attribution - NonCommercial 4.0 International License

Version of Record: https://www.sciencedirect.com/science/article/pii/S2329050119300944
Manuscript_984730bc41efa55bb08a09f5cd8a1e91

Role of regulatory T cells and effector T cell exhaustion in liver-mediated transgene tolerance in muscle

Jérôme Poupiot[1], Helena Costa Verdera[2], Romain Hardet[2], Pasqualina Colella[1], Fanny Collaud[1], Laurent Bartolo[3], Jean Davoust[3], Peggy Sanatine[4], Federico Mingozzi[4*], Isabelle Richard[1*] and Giuseppe Ronzitti[1*†]

[1] INTEGRARE, Genethon, Inserm, Univ Evry, Université Paris-Saclay, 91002, Evry, France

[2] UPMC, 75005, Paris, France

[3] UMR 1151, Necker - Institut Enfants Malades – Molecular Medicine Center

[4] Genethon, Evry, France

* These authors contributed equally to this work

† correspondence should be addressed to;

Dr. Giuseppe Ronzitti

1bis rue de l'internationale

91000 Evry

gronzitti@genethon.fr

© 2019 published by Elsevier. This manuscript is made available under the CC BY NC user license
https://creativecommons.org/licenses/by-nc/4.0/

Abstract:

The pro-tolerogenic environment of the liver makes this tissue an ideal target for gene replacement strategies. In other peripheral tissues such as the skeletal muscle, anti-transgene immune response can result in partial or complete clearance of the transduced fibers. Here, we characterized liver-induced transgene tolerance after simultaneous transduction of liver and muscle. A clinically relevant transgene, α-sarcoglycan, mutated in limb-girdle muscular dystrophy type 2D, was fused with the SIINFEKL epitope (hSGCA-SIIN) and expressed with adeno-associated virus vectors (AAV-hSGCA-SIIN). Intramuscular delivery of AAV-hSGCA-SIIN resulted in a strong inflammatory response, which could be prevented and reversed by concomitant liver expression of the same antigen. Regulatory T cells and upregulation of checkpoint inhibitor receptors were required to establish and maintain liver-mediated peripheral tolerance. This study identifies the fundamental role of the synergy between Tregs and upregulation of checkpoint inhibitor receptors in the liver-mediated control of anti-transgene immunity triggered by muscle directed gene transfer.

Introduction

The liver is one of the body's main biosynthetic organs, with key detoxifying functions enabled by an efficient access to the systemic blood circulation and an intense metabolic activity. These characteristics make the liver an ideal target for gene replacement strategies. Results from clinical trials in hemophilia A and B support this point, establishing the safety and the efficacy of adeno-associated virus (AAV) vector-mediated gene transfer to human hepatocytes.[1, 2] Another important feature of the hepatic environment is related to its pro-tolerogenic properties, initially described in the context of organ transplant.[3] This is consistent with the fact that liver, together with intestine, is the primary site of antigen presentation for food-derived proteins, and the presence of cells specialized in the control of immune responses results in what is known as an immune privileged status. As a result, different hepatotropic viruses exploit the pro-tolerogenic milieu of the liver to persist and cause chronic diseases.[4]

Several mechanisms were reported to be responsible for the tolerogenic properties of the liver, e.g. the secretion of the pro-tolerogenic cytokines IL-10 and TGFβ by specialized antigen presenting cells, the upregulation of inhibitory co-receptors, and the expansion of regulatory T cells (Tregs).[5] Tregs have a primary role in the control of humoral and cell-mediated immune responses against vector-encoded transgenes observed after liver gene transfer.[6, 7] However, in the context of anti-transgene cytotoxic immune response, mechanisms other than Tregs induction are likely to be involved in the control of the immune response.[8]

Inhibitory co-receptors are part of a large family of co-receptors with a negative function on the activation of immune responses. After activation, the levels of these molecules on the surface of the immune cells increase, reflecting their role in the fine tuning of the immune reactions to antigens. The impact of the expression of these molecules in the control of

immune responses is particularly evident in chronic liver infections[9] and in tumors[5], in which the expression of inhibitory co-receptor ligands mediates immune escape. A possible role for inhibitory co-receptors in the modulation of anti-transgene cytotoxic immune response via liver gene transfer has been hypothesized, although a direct characterization of the phenomenon is still missing.[10, 11]

Differently from what observed in liver,[6, 12, 13] AAV-mediated gene transfer after intramuscular injection may result in the development of anti-transgene immune responses.[14] Expansion of antigen-specific CD8+ T cells has been associated with the clearance of transduced fibers both in preclinical and clinical studies.[15-17] Like in the case of muscular dystrophies, in which Tregs have been documented to home to the inflamed muscle,[18, 19] AAV-triggered cytotoxic immune responses are balanced by Tregs able to partially control anti-transgene immune responses.[20] Early findings demonstrated that the simultaneous liver and muscle targeting is able to control the humoral and cell mediated anti-transgene immune responses.[21, 22]

Here, we characterized the liver-mediated control of anti-transgene immune response resulting from the intramuscular injection of an AAV vector expressing human α-sarcoglycan (hSGCA). This protein, mutated in limb-girdle muscular dystrophy type 2D, when expressed in $Sgca^{-/-}$ muscle, induces a strong anti-transgene immune response resulting in fiber loss and transgene clearance.[23]

We found that concomitant liver and muscle expression of hSGCA was able to control the anti-transgene immune response even when this immune response was established ahead of liver gene transfer. Then, using a model antigen derived from hSGCA, we characterized in detail the cytotoxic anti-transgene immune response. Importantly, by taking advantage of antibodies specifically depleting Tregs or inhibiting the interactions between inhibitory co-

receptors and their ligands, we dissected the synergistic role of these mechanisms in the control of the immune response in the setting of concomitant AAV-mediated liver and muscle gene transfer.

Results

Liver gene transfer controls cytotoxic transgene-specific immune responses resulting from intramuscular injection in dystrophic mice.

AAV-mediated liver gene transfer induces a strong peripheral tolerance likely to control the anti-transgene immune responses at a systemic level.[12, 24] Here, we challenged the robustness of this mechanism in a dystrophic mouse model characterized by muscle inflammation and known to mount significant immune responses against the human SGCA protein.[25] *Tibialis anterior* (TA) muscle of $Sgca^{-/-}$ mice were injected intramuscularly (IM) with vehicle (PBS, Control group) or with an AAV6 vector expressing human α-sarcoglycan (hSGCA) under the control of the muscle promoter SPc5.12. Five days later, mice received by a systemic route either empty AAV9 capsids (Muscle group) or an AAV9 vector expressing the hSGCA transgene under the control of human alpha-1-anti-trypsin (hAAT) liver specific promoter (Muscle-Liver group, **Fig.1A**). Two months after vector injection, the expression of hSGCA transgene in the liver of Muscle-Liver injected animals was confirmed by reverse transcription quantitative PCR (RT-qPCR) and immunostaining (**Supplementary Fig. 1A,B**). A significant enhancement in muscle transduction and consequent muscle structure normalization was observed in Muscle-Liver group compared to Muscle group as shown by immunohistochemistry (**Fig.1B)**, anti-hSGCA immunostaining (**Fig.1C)** and miR206 expression (**Fig. 1D**), a marker of regeneration in muscle.[26] The quantification of the vector genome copy number (VGCN) per diploid genome confirmed the improved transduction in muscle of animal of the Muscle-Liver group ($p<0.01$ vs. Muscle group, **Fig. 1E**). Animals receiving the vector intramuscularly (Muscle group) also developed a robust anti-hSGCA humoral immune response, which was significantly reduced in the Muscle-Liver treated group ($p<0.05$, **Fig.1F**). The inhibition of the anti-hSGCA humoral response was associated with a reduction of activated CD8+ cells infiltrating the injected muscle of Muscle-Liver -treated

animals, as confirmed by immunohistochemistry (**Fig. 1C**) and mRNA expression of inflammatory markers CD8 and IFNγ in the same group (**Fig. 1G,H**, $p<0.001$ and $p<0.05$ vs. Muscle, respectively). Increased secretion of IFNγ from hSGCA protein-stimulated splenocytes extracted from mice of Muscle group compared to Muscle-Liver group ($p<0.05$, **Fig.1I**) was also observed.

These results demonstrate that liver gene transfer induces a dominant peripheral tolerance to a human transgene expressed in a dystrophic muscle. This represents a particularly stringent setting as the fragility of the muscle fibers, consequent to the lack of SGCA protein in the dystrophin complex, induces a persistent inflamed state in the muscle that enhances anti-transgene immune responses.[17, 27]

Liver expression of hSGCA prevents and reverses the loss of transduced fibers in muscle of wild-type mice

To evaluate whether wild-type mice had an anti-hSGCA immune response similar to that observed in KO animals, eight week-old C56BL6 mice were injected intramuscularly with a vector expressing hSGCA under the control of the SPc5.12 promoter (**Supplementary Fig. 2A**). Mice were sacrificed 5, 15 and 30 days after vector injection. Histological analysis indicated the presence of CD8+ T cell infiltrates in the muscle, consistent with an ongoing immune response (**Supplementary Fig. 2B**). CD8 mRNA levels in muscle extracts were increased compared to PBS-injected mice at day 15 and 30 ($p<0.001$ vs. CTRL), whereas IFNγ mRNA levels were increased 15 days after vector injection ($p<0.0001$ vs. CTRL, **Supplementary Fig. 2C,D**). Decreased VGCNs were observed 15 and 30 days after vector injection ($p<0.0001$ vs. D5), suggesting that the ongoing transgene immune response resulted in clearance of the vector from transduced muscle fibers (**Supplementary Fig. 2E**). Of note, a separate control cohort of mice injected with an AAV6 vector expressing murine secreted

alkaline phosphatase at the same dose did not show any sign of inflammation (data not shown). These results suggest that AAV-mediated expression of hSGCA is immunogenic in wild-type mice regardless of the endogenous expression of murine SGCA.

The presence of an immune response in wild-type mice offered the possibility to investigate the liver-mediated control of the anti-hSGCA immune response without the confounding effect of immune signals due to the dystrophic process ongoing in $Sgca^{-/-}$ mice. C57BL/6J mice were injected IM with an AAV6-SPc5.12-hSGCA vector and then received a systemic injection of an AAV9 vector expressing the same transgene under the transcriptional control of the liver-specific promoter hAAT. This second vector administration was performed either on the same day (Muscle-Liver D0) or 15 days after (Muscle-Liver D15) IM injection (**Fig. 2A**) at the peak of muscle inflammation as observed in Supplementary figure 2. One month after vector injection, hSGCA was expressed in the liver of mice of the Muscle-Liver D0 and D15 groups at similar levels (**Supplementary Fig. 2F**). As expected, animals injected intramuscularly with the AAV6-SPc5.12-hSGCA vector alone showed increased levels of CD8+ infiltrates whereas the concomitant systemic injection of the liver-expressing vector reduced the level of infiltrates, in particular when the two vectors were administered at the same time point (**Fig. 2B**). Analysis of the levels of expression of CD8 mRNA in the muscle confirmed the reduction of CD8 expressing cells in mice co-injected in muscle and liver at day 0 ($p<0.01$ vs. Muscle group), but not at day 15 (**Fig. 2C**). Interestingly, the levels of IFNγ mRNA were similar between Muscle-Liver D0 and D15 groups and significantly reduced compared to the Muscle group ($p<0.05$, **Fig. 2D**). The decreased immune reaction was associated with an improved transduction of muscle fibers of mice of the Muscle-Liver D0 and D15 groups as measured by VGCN analysis ($p<0.001$ and $p<0.05$ vs. Muscle only, respectively, **Fig. 2E**).

We then measured the levels of expression of a panel of mRNAs of immune-related genes in the liver of treated mice (**Supplementary Table 1**). Consistent with previous reports of antigen-independent homing of activated T cells in the liver,[28] CD4 mRNA levels were significantly increased in liver of mice IM-treated with the AAV6- SPc5.12-hSGCA vector, which experienced the highest inflammation levels. Conversely, in mice treated with both muscle and liver vectors simultaneously or 15 days apart, the upregulation of genes associated with tolerance and T cell exhaustion such as Fox-P3 and PD-L1 was noted as well as the increase of CD8 expression suggesting homing of CD8 T cells in the liver(**Supplementary Table 1**).

These data confirm that liver-targeted expression of hSGCA is able to control the induction of anti-hSGCA immune response following intramuscular administration. Importantly, the results for the D15 group indicate that liver transduction is able to control, at least partially, an already-established immune response. Liver T cell homing and upregulation of immunomodulatory genes appear to be signatures of the phenomenon.

Muscle expression of the SIINFEKL-hSGCA fusion protein is highly immunogenic and allows tracking transgene-specific T cell responses

Based on the results in $Sgca^{-/-}$ and wild-type mice, we then better characterized the cytotoxic response to the hSGCA transgene. To evaluate the activation of antigen-specific T cells, we fused the C-terminal of the protein with a portion of the ovalbumin protein containing the MHC class I-specific[29] epitope SIINFEKL (hSGCA-SIIN, **Fig. 3A**). As a control of the specificity of the immune response, hSGCA was fused with a scrambled version of the SIINFEKL peptide, FILKSINE (hSGCA-FILK). C57BL/6J mice were injected intramuscularly with AAV1 or AAV6 vectors expressing hSGCA or with AAV1 vectors expressing hSGCA-SIIN or hSGCA-FILK under the control of the SPc5.12 promoter (**Fig.**

3B). Fifteen days after the injection, mice were sacrificed and the activation of T-cells was tested by IFN-γ ELISPOT. As expected, the stimulation of splenocytes with the SIINFEKL peptide led to a robust activation in mice injected with AAV1 vectors expressing hSGCA-SIIN but not with hSGCA-FILK ($p<0.05$ vs. CTRL, **Fig. 3C**). When the stimulation was performed with the hSGCA recombinant protein (**Fig. 3D**) we observed a robust T-cell activation only in the group injected with the SGCA-SIIN antigen ($p<0.05$ vs. CTRL, respectively). Interestingly, the stimulation with a peptide epitope derived from hSGCA and predicted to bind to MHC class I (**Fig. 3E** and **Supplementary Fig. 3**), induced a general increase in the IFNγ ELISPOT spot counts in all the groups injected with vectors expressing hSGCA. However, statistical significance was reached only in the group injected with the hSGCA-SIIN fusion protein ($p<0.01$ vs. CTRL, respectively). No differences were observed between AAV1 and AAV6 serotypes. The injection of the hSGCA-SIIN-expressing vector also resulted in increased muscle CD8+ T cell infiltrates as visualized by hematoxylin phloxine saffron (HPS) staining and immunofluorescence (**Fig. 3F**). These results were also confirmed by the increased levels of CD8 and IFN-γ mRNA in the hSGCA-SIIN injected muscle ($p<0.0001$ and $p<0.05$ vs. CTRL, respectively, **Fig. 3G,H**). These results indicate that the hSGCA-SIIN fusion protein is highly immunogenic and allows tracking of transgene-specific immune responses both to SIINFEKL and hSGCA. Fifteen days after the IM injection of the hSGCA-SIIN expressing AAV1 vector, we observed a significant decrease in the levels of hSGCA expressed in the injected muscle ($p<0.05$ vs. AAV1-FILK) to levels undistinguishable from PBS-injected mice (**Fig. 3I**). These data confirm the immunogenicity of the hSGCA in wild-type mice regardless of the expression of the endogenous murine protein. They also indicate that the hSGCA-SIIN transgene is functionally expressed in muscle fibers and represents a tool to measure immune response activation both against SIINFEKL and MHC class I epitopes derived from hSGCA.

Local changes in liver T cell populations are associated with the suppression of anti-hSGCA-SIINFEKL immune responses

To evaluate if concomitant liver and muscle transduction was able to prevent the anti-transgene cytotoxic response, C57BL/6J mice were injected intramuscularly with an AAV1 vector expressing hSGCA-SIIN and intravenously with an AAV9 vector expressing the same transgene under the control of a liver-specific promoter (Muscle-Liver group) (**Fig. 4A**). As controls, mice were injected with PBS (Control), or intramuscularly with an AAV1 vector expressing hSGCA-SIIN (Muscle group), or intravenously with an AAV9 vector expressing the same transgene in hepatocytes (Liver group). One month post-injection, activation of T-cells was measured with an IFN-γ ELISPOT assay, showing the formation of positive spots in the Muscle group only ($p<0.05$ vs. all groups, **Fig. 4B**). Similarly, animals receiving the vector intramuscularly (Muscle group) developed a robust anti-hSGCA humoral immune response ($p=0.0253$ vs. Control, **Fig. 4C**), which was absent in both Liver and Muscle-Liver treated groups. In Muscle-Liver group, the lack of T-cell activation in splenocytes was accompanied by an increased number of AAV genome copies in the injected muscle ($p<0.05$ vs. Muscle group, **Fig. 4D**), and a decreased expression of CD8 and IFN-γ mRNA in the same group ($p<0.05$ vs. Muscle group for CD8, **Fig. 4E,F**). The evaluation of the expression of Treg-signature genes showed increased levels of expression of FoxP3, IL10 and GITR in the Muscle group ($p<0.05$ vs. CTRL group, **Supplementary Table 2**). Interestingly, the levels of expression of amphiregulin (AREG), a growth factor expressed by muscle Tregs[19] were increased only in the Muscle liver group ($p<0.01$ vs. CTRL group, **Supplementary Table 2**). When we evaluated the expression of hSGCA and the presence of CD8+ T cell infiltrates by immunofluorescence, we confirmed the reduction of infiltrates and the improved muscle transduction in the Muscle-Liver group (**Fig. 4G**). As expected, VGCN analysis in liver showed similar transduction in Liver and Muscle-Liver groups (**Fig. 4H**). Notably, no

inflammation was observed in the liver after gene transfer as measured by the level of expression of CD8 and IFN-γ mRNA in this tissue (**Fig. 4I,L**). The activation of CD8+ T cells was also evaluated in splenocytes by flow cytometry using a SIINFEKL-specific MHC class I dextramer. In the Muscle group, a significant increase in the number of circulating, activated CD8+CD44+ T cells specific for SIINFEKL was reported ($p<0.05$ vs. all groups, **Supplementary Fig. 4A,B**). Similarly, an increase in Dextramer+ CD8+ cells was observed in non-parenchymal cells extracted from livers of the Muscle group (**Supplementary Table 3**). In mice injected with the combination of the two vectors (Muscle-Liver), the number of activated SIINFEKL-specific CD8+ T cells both circulating and infiltrating the liver was undistinguishable from that measured in the untreated control group (**Supplementary Fig. 4A-E** and **Supplementary Table 3**). These results indicate that liver transfer of the transgene concomitant to muscle injection controls the anti-hSGCA-SIIN immune response.

Next, based on the RNA expression data in the liver of Muscle-Liver-treated wild-type mice (**Supplementary Table 1**), and on published literature on the possible role of Tregs and exhaustion of activated T cells in liver tolerance [5], we further investigate the fate of regulatory and effector T cells in the liver of treated animals by flow cytometry. We observed a significant increase of CD4+ FoxP3+ Tregs in both Liver and Muscle-Liver groups ($p<0.05$ vs. Control, **Fig. 5A,B**). Interestingly, the levels of CD8+ T cells positive for PD-1 were significantly increased only in the Muscle-Liver group ($p<0.05$ vs. Control, **Fig. 5C,D**) and 18.3% of them were positively stained with the SIINFEKL-specific MHC class I dextramer (**Supplementary Fig. 4C** and **Supplementary Table 3**). Of note, 65% and 56% of PD-1 positive CD8 T cells isolated from livers of the Muscle-Liver group were also positive for LAG3 ($p<0.01$ vs. ontrol, **Fig. 5E,F**) and TIM3 ($p<0.05$ vs. Control, **Fig. 5G,H**) respectively. Of those cells, between 6% and 8% were positively stained with the SIINFEKL-specific MHC class I dextramer (**Supplementary Fig. 4D, E**). In splenocytes, no changes in Tregs

(**Supplementary Fig. 4F,G**), PD-1 CD8+ T cells or double-positive PD-1/LAG3 and PD-1/TIM3 CD8+ T cells were noted (**Supplementary Fig. 4H,I**).

These data confirm the role of Tregs in the liver-mediated control of anti-transgene immune response. The simultaneous expression of PD-1/LAG3 and PD-1/TIM3 in liver intraparenchymal, antigen specific CD8+ T cells observed only in the Muscle-Liver group was associated with the lack of inflammation in the liver. This suggests that the exhaustion of transgene-specific CD8+ T cells, homing to the liver, may play a role in the hepatic control of immune response when immunogenic transgenes are expressed in muscle.

Immune-checkpoint blockade fails to break liver-induced tolerance

To further investigate the role of T cell exhaustion in liver-mediated control of anti-transgene immunity in muscle, we took advantage of antibodies specifically blocking the interaction between inhibitory co-receptors and their ligands.[30] Specifically we evaluated the simultaneous blockade of the PD-1/PD-L1 pathway in combination with LAG3 inhibition. C57BL/6J mice, injected intramuscularly with an AAV1 vector expressing hSGCA-SIIN and intravenously with an AAV9 vector expressing the same transgene under the control of a liver specific promoter, received 5 intraperitoneal injections of the combination of 200 μg/mouse of anti-PD1, anti-PDL1 and anti-LAG3 antibodies (Muscle-Liver +Ab) or five injections of PBS (Muscle-Liver) at the indicated time points (**Fig. 6A**). Additional controls included mice injected either with PBS (Control) or intramuscularly with AAV1 expressing hSGCA-SIIN (Muscle). Fifteen days after vector injection, T cell activation was measured by IFN-γ ELISPOT. A significant increase in the number of spots was counted in splenocytes obtained from mice in the Muscle group re-stimulated with SIINFEKL peptide ($p<0.0001$ vs. all groups, **Fig. 6B**). In the Muscle-Liver +Ab group, we observed a slight increase in the spot count, although not statistically significant (**Fig. 6B**). These results were confirmed by flow

cytometry using MHC class I SIINFEKL-specific dextramer, which showed a significant increase in the number of CD8+CD44+Dextramer+ splenocytes only in mice from the Muscle group ($p<0.05$ vs. all groups, **Supplementary Fig. 5A,B**). In agreement with the ELISPOT results, CD8+ T cell immunofluorescent staining showed a slight increase in T cells infiltrates in muscle of mice of the Muscle-Liver +Ab group (**Fig. 6C**). Similarly, CD8, IFN-γ and FoxP3 mRNA levels were increased in the Muscle group ($p<0.05$ vs. all groups for CD8, **Supplementary Fig. 5C,D,E**), while a small, not significant, increase was noted in in the Muscle-Liver +Ab group (**Supplementary Fig. 5C,D,E**). No differences were reported in the vector genome copy number between Muscle-Liver and Muscle-Liver+Ab groups (**Supplementary Fig. 5F**).

As expected, anti-hSGCA humoral immune response was significantly increased only in animals receiving the vector intramuscularly (Muscle group, $p=0.0244$ vs. Control, **Supplementary Fig. 5G**). Animals receiving vectors both in muscle and liver and treated with the combination of anti-PD1, anti-PDL1 and anti-LAG3 antibodies (Muscle-Liver +Ab) showed increased anti-hSGCA humoral immune response compared to Muscle-Liver group although the difference did not reach statistical significance.

Analysis of liver T cell infiltrates revealed an increase of CD8+ T cells in Muscle-Liver +Ab animals (**Fig. 6D**), and a significant upregulation of CD8 and IFN-γ mRNA expression ($p<0.01$ vs. all groups, **Supplementary Fig. 5H,I**). Interestingly, this was accompanied by an increase in FoxP3+ T cells detected by immunofluorescence (**Fig. 6E**) and FoxP3 mRNA levels ($p<0.01$ vs. all groups, **Supplementary Fig. 5L**) in liver. The increase in FoxP3+ T cells infiltrates in the liver in the Muscle-Liver +Ab group was also confirmed by flow cytometry ($p<0.001$ vs. all groups, **Fig. 6F,G**).

These results indicate that immune-checkpoint blockade alone was not sufficient to break liver tolerance. They also suggest a compensatory role of Tregs in the liver, possibly accounting for the suppression of effector T cells expanded following immune-checkpoint blockade.

Concomitant Tregs depletion and immune-checkpoint blockade restores anti-SIINFEKL cytotoxicity and break liver tolerance

To identify any possible synergy between Tregs and T cells exhaustion in the liver-mediated control of the anti-SIINFEKL immune response in muscle, we injected intramuscularly C57BL/6J mice with an AAV1 vector expressing hSGCA-SIIN and intravenously with PBS (Muscle) or an AAV9 vector expressing the same transgene under the control of the hAAT promoter. Mice received 3 intraperitoneal injections of an anti CD25 antibody (250 µg/mouse) for Tregs depletion and 5 intraperitoneal injections of the combination of 200 µg/mouse of anti-PD1, anti-PDL1 and anti-LAG3 antibodies (Muscle-Liver -Treg+Ab) or 3 intraperitoneal injections of an anti CD25 antibody at the dose of 250 µg/mouse (Muscle-Liver -Treg) or five injections of PBS (Muscle-Liver) at the indicated time points (**Fig. 7A, B**). As expected, in Muscle group we observed the largest number of IFN-γ positive spots as measured by ELISPOT ($p<0.05$ vs Muscle-Liver, **Fig.7C**). Interestingly, a significant increase in the number of IFN-γ positive spots in splenocytes from mice of the Muscle-Liver -Treg+Ab group ($p<0.05$ vs Muscle-Liver, **Fig.7C**) was observed. At the same time, CD8+ T cell infiltrates were detected in liver both by flow cytometry and immunofluorescence ($p<0.05$ vs. Muscle-Liver, **Fig.7D** and **Supplementary Fig. 6A**, respectively) in livers. Additionally, a significantly elevated frequency of CD8+CD44+Dex+ T cells was detected by flow cytometry in non-parenchymal liver cells extracted from mice of the Muscle and the Muscle-Liver -Treg+Ab groups ($p<0.05$ vs. Muscle-Liver, **Fig. 7E,** and **Supplementary Fig. 6B**). Simultaneous Tregs depletion and PD1/PDL1/LAG3 blockade also resulted in decreased

vector copies in injected muscle ($p<0.05$ vs. Muscle-Liver, **Fig.7F**), increased CD8+ T cell infiltrates co-localized with fibers expressing the hSGCA transgene, as observed by immunofluorescence (**Fig.7G**). CD8 and IFN-γ mRNA expression was also significantly upregulated in muscle ($p<0.05$ vs. Muscle-Liver for CD8, $p<0.05$ vs. Muscle-Liver -Treg for IFNγ, **Supplementary Fig. 6C, D**). Accordingly, although the anti-hSGCA humoral response was reduced in mice of the Muscle-Liver and Muscle-Liver -Treg groups ($p=0.0453$ and $p=0.0107$ vs. Muscle group, respectively), when both Tregs depletion and PD1/PDL1/LAG3 blockade were applied, the anti-hSGCA antibodies were not significantly different from the one measured in mice of the Muscle group ($p=0.2164$ vs. Muscle group, **Supplementary Fig. 6E**). These results demonstrate that Treg depletion alone cannot break an already established tolerance and that PD1/PDL1 and LAG3 acts synergistically with Tregs induction in maintaining liver-dependent anti-transgene tolerance and controlling transgene-specific T cell responses in muscle.

Discussion

Muscle can be considered the hotbed of immune responses, particularly when underlying conditions alter its immune environment.[31] This poses important challenges to the development of gene transfer strategies for the treatment of neuromuscular diseases, particularly for muscular dystrophies, in which continuous muscle breakdown and regeneration trigger inflammation. Here, we dissected the role and mechanisms of liver-mediated control of transgene immune responses induced by muscle-directed gene transfer with AAV vectors. This work highlights the synergy between liver-induced regulatory T cells and inhibitory co-receptors, involved in the control of effector T cell responses, in preventing and reversing cell-mediated transgene immunity in muscle.

Preclinical and clinical results of AAV vector-based gene therapies for neuromuscular disorders indicate that intramuscular delivery of AAV vectors is likely to trigger both humoral and cell-mediated transgene immune responses.[14-17] Several factors contribute to shape the magnitude of these responses; for example, host genetic background,[32] underlying muscle inflammation,[17, 33] and pre-existing immunity to the encoded transgene,[34] can exacerbate transgene immunity and result in loss of transduced muscle fibers.[17] Interestingly, experience with AAV vector mediated muscle gene transfer in small and large animal models indicate that there is a direct relationship between transgene immunogenicity and route of vector administration. While intramuscular delivery of AAV vectors triggers robust immune responses, systemic vector administration is associated with low to absent anti-transgene immunogenicity.[35, 36] While the outcome of muscle-directed gene transfer could be inferred to differences in antigen presentation in intramuscular vs. systemic gene transfer (i.e. local expression of an antigen at high levels via intramuscular vector delivery is more immunogenic than widespread and uniform expression of the same transgene[37]), it is likely that concomitant

liver and muscle transduction achieved via systemic vector delivery mediates efficient transgene acceptance.[21, 22]

Starting from these observations, and based on the extensive body of work related to hepatic-induced transgene tolerance,[6-8, 38-40] here we characterized the mechanisms involved in the control of cytotoxic T cell responses and possibly mediating transgene acceptance after systemic gene delivery.

Liver-mediated induction of immunological tolerance was first described in the context of AAV gene transfer for coagulation factor IX (F.IX)[41] and subsequently with other vector platforms[42] and transgenes.[43, 44] Interestingly, liver mediated expression of a transgene has been shown to prevent both humoral and cell-mediated responses triggered by various immunization methods.[22, 24, 38-41] In the setting of established humoral immune responses, liver expression has been shown to be effective in the eradication of antibodies to F.IX and coagulation factor VIII, among other antigens, in both small and large animals.[13, 44] Here, we show that liver tolerance is highly effective also in the setting of an ongoing distructive T cell response directed against the transgene, as we were able to rescue transgene expression even when the tolerogenic liver transgene expression was instated two weeks after the immunogenic intramuscular vector delivery. This is a fundamentally important finding in the treatment of neuromuscular diseases, in particular muscular dystrophies, in which muscle inflammation and pre-existing T cell immunity to the therapeutic transgene can hinder the efficacy of gene transfer.[17, 34]

The mechanisms described as mediating hepatic tolerance in the context of AAV gene transfer are multiple,[8, 10] although regulatory T cells appear to be key mediators of the suppression of effector T cell responses,[6, 7] as depletion of Tregs at the time of gene transfer results in induction of transgene-directed immune responses.[12, 45]

The present work, in which the therapeutically-relevant transgene α-sarcoglycan was used as a model, supports the hypothesis that effector T cell homing to the liver and their subsequent expression of the checkpoint markers PD1 and LAG3 on CD8+ T cells is associated with the induction of transgene tolerance and synergistic with the induction of Tregs in controlling anti-transgene immunity. Exhaustion is specifically involved in the control of the immune response when the transgene is expressed in both muscle and liver, and blockade of PD1 and LAG3 is key required to break tolerance. These results are consistent with our recent work in which the ovalbumin model antigen was used to study liver-induced muscle tolerance,[46] and provide additional mechanistic insights on the role of effector T cell homing to the liver and subsequent expression of checkpoint markers for the control of transgene immunogenicity.

Antigen levels in liver play a central role in shaping local immune responses to antigens, as demonstrated in the context of hepatic expression of FIX[41] and ovalbumin.[10, 11] As shown here, the fusion of the ovalbumin SIINFEKL epitope, with high affinity for MHC class I, to α-sarcoglycan allowed for the detection of effector T cells by ELISPOT and MHC class I detramer. Likely due to a bystander effect, it also enhanced the detection of immune responses specific for hSGCA in the ELISPOT assay. Thus, the hSGCA-SIIN fusion represents a tool to monitor transgene-specific immune responses which could be used develop new strategies to control anti-transgene immune responses in the context of animal models of muscular dystrophies, aimed at improving the safety and efficacy of gene transfer. However, a potential drawback of the strategy used here is that the fusion of immunogenic peptides, accelerate the kinetic of the formation of the immune response and it is likely to modify both the mechanism of tolerance formation and the levels of antigen needed to establish and maintain the peripheral tolerance.

Future work will be aimed at carefully dissecting and comparing the mechanisms involved in the induction of tolerance against hSGCA and hSGCA-SIIN and at determining the minimal

levels of liver expression necessary to prevent muscle-induced transgene immune responses in the context of low- or high- affinity MHC class I epitopes. To this aim, recent work from our lab, in the context of Pompe disease gene therapy, shows that the combination of strong liver promoters with muscle promoters results in good control of anti-transgene immune responses, while weaker liver expression fails to control muscle-driven anti-transgene humoral response.[21]

Reversal of established humoral immunity to a variety of therapeutic transgenes has been demonstrated in small[47, 48] and large[13, 44] animal models of gene transfer. Here, we show the control of an already established CD8+ T cell response against hSGCA mediated by both the induction of Tregs and the homing of transgene-specific CD8+ T cells to the liver, where they express PD1 and LAG3. The exact mechanism driving homing of reactive CD8+ T cells to the liver remains to be elucidated, although recent work from Paul-Heng and colleagues[49] suggest that direct recognition of antigen expressed in the liver by CD8+ T cells via MHC class I is a key mediator of liver tolerance. Thus, it is conceivable that homing of reactive CD8+ T cells to the liver, via MHC class I recognition of the expressed transgene, together with the unique protolerogenic hepatic immune environment, results in the control of cytotoxic responses via T cell exhaustion. To this end, one interesting and unique finding of the current work is that immune checkpoint blockade alone is ineffective in breaking liver-induced tolerance. Following the administration of antibodies against PD1, PDL1, and LAG3[50], given at the time of vector infusion, a slight increase in infiltrating CD8+ T cells was seen in both muscle and liver of animals. At the same time, Tregs were also found in greater number in the same tissues, with no loss of transgene expression of vector genome copy number. This compensatory phenomenon could be explained simply by Tregs homing to the inflamed tissue, like it has been seen in muscle[18, 19] and liver,[51] or could simply reflect effect

of enhanced proinflammatory signals on Tregs homeostasis.[52] Careful phenotyping of regulatory T cells infiltrates will provide a better understanding of this observation.

The fact that the restoration of transgene immune responses after combined Tregs depletion and checkpoint inhibition blockade was only partial may suggest the existence of additional mechanisms mediating liver tolerance. Alternatively, the anti-CD25 antibody (clone PC-61.5.3) used to depleted Tregs may have affected activated effector T cells expressing the CD25 marker.

The working hypothesis to explain the findings presented here is that, in the absence of liver transduction, CD8+ cells primed in the draining lymph nodes, home to the muscle where they sustain inflammation and clear the transgene expressed in AAV-transduced muscle fibers. Following intramuscular gene transfer, transgene-specific T cells can home to the liver, however in the absence of transgene expression in hepatocytes no suppression of the immune response occurs (**Supplementary Fig. 7A**). When the hSGCA transgene is expressed in the liver, reactive T cells infiltrating the liver are suppressed by the synergistic action of Tregs and upregulation of the inhibitory receptors PD1/PD-L1 and LAG3. T cells homing to the liver in this case do not participate to the ongoing inflammation in the muscle and the net result is reduced immune response (**Supplementary Fig. 7B**). Simultaneous inhibition of the PD1/PD-L1/LAG3 pathways, together with Treg depletion, lead to the re-activation of exhausted cells that participate in the immune response against the transgene occurring in muscle (**Supplementary Fig. 7C**). The mechanism proposed represents a simplified model because it excludes the tolerance mechanisms acting locally in the muscle that participate in the control of the anti-transgene immune response.[31]

In conclusion, concomitant liver and muscle expression via AAV vectors allows for efficient prevention and eradication of transgene-specific humoral and cell-mediated immune

responses, resulting in long-term transgene expression. Induction of Tregs and effector T cell exhaustion are both key requirements for the effective hepatic control of immune responses. This work provides further insight on the mechanisms of liver-induced immunological tolerance; it also has direct implications on the design of transgene expression cassettes[21] when aiming to treat neuromuscular diseases with underlying muscle inflammation.

Materials and Methods

Study approval

Animal studies were performed in accordance with the current European legislation on animal care and experimentation (2010/63/EU) and approved by the institutional ethics committee of the CERFE in Evry, France (protocol DAP2015-003-A).

Animal models

The following mouse strains were used: C57BL/6J, and Sgca$^{-/-}$ mice. Sgca$^{-/-}$ mice were bred in a pure C57BL/6J background by crossing 10 times in C57BL/6J background.

AAV-mediated gene transfer

AAV vectors production was performed as already described.[53] Three different serotypes of recombinant adeno-associated virus 1, 6 and 9 (AAV1, AAV6, AAV9) vector were used to restore α-sarcoglycan expression in muscle of Sgca$^{-/-}$ mice. The use of AAV1 and 6 for muscle gene transfer was motivated by their poor humoral cross-reactivity that allowed for 15-day delayed administration of the AAV9 after intramuscular injection of AAV1 and 6 (data not shown) and also by the low leakage in circulation of these serotypes after intramuscular administration.[54] The use of AAV9 for liver gene transfer was also justified by the fact that liver transduction with this serotype resulted in efficacy similar to what observed with AAV8, a classical serotype for liver targeting in both murine models and humans.[55] Viral genomes were quantified by a TaqMan™ real-time PCR assay using the following primer pairs and TaqMan™ probes: Fwd: 5'-CTCCATCACTAGGGGTTCCTTGTA-3'; rev: 5'-TGGCTACGTAGATAAGTAGCATGGC-3'; Probe: 5'-GTTAATGATTAACCC-3'. Mice were injected intravenously into the tail vein with a standard volume of 200 µl of either PBS

or AAV9. Intramuscular injections of AAV1 or AAV6 vectors were performed by injection of 25µL of the diluted vector in the left *Tibialis Anterior* (TA) muscle.

Liver intra-parenchymal cells and splenocytes extraction

Liver intra-parenchymal cells were isolated by mechanical dissociation of the liver tissue and differential centrifugation. Briefly, livers were dissociated using a 70 µm cell strainer (Thermo Fisher Scientific, Waltham, MA) and centrifuged 5 minutes at 300 x g to remove hepatocytes and tissue debris. Supernatant were then centrifuged 10 minutes at 500 x g. The pellet of this second centrifugation was resuspended in 40% Percoll and overlayed on a 70% Percoll cushion. After centrifugation for 25 minutes at 1400 x g, the non-parenchymal cells were recovered at the interface between the two layers and used for staining.

Splenocytes were freshly isolated from mouse spleen by mechanical dissociation using a 70 µm cell strainer (Thermo Fisher Scientific, Waltham, MA) and centrifugation 10 minutes at 500 x g to recover the cells.

Histological and immunohistochemistry analyses

Eight micrometers transversal cryosections were cut from liquid nitrogen-cooled isopentane frozen TA muscles or livers and stained following classical protocols for histology coloration and immunohistochemistry. Sections were processed for hematoxylin phloxine saffron (HPS) staining as already described and visualized on a Nikon Eclipse E600 microscope (Nikon, Minato, Tokyo, Japan). For immunostaining, unfixed, transverse cryosections were first blocked with PBS containing 20% Fetal calf serum (FCS) for 1 h and then incubated with primary antibodies overnight at 4°C. For the detection of hSGCA expressing fibers and CD8 T cells, a rabbit polyclonal primary antibody directed against amino acids 366–379 of the human α-sarcoglycan sequence (AC-ahSarco57, Eurogentec, Seraing, Belgium) and a rat-anti

CD8α (Thermo Fisher Scientific, Waltham, MA) were used. For the detection of Foxp3 and CD3 infiltrating cells in liver, TA sections were incubated with a rat anti-Foxp3 (eBioscience, Thermo Fisher Scientific, Waltham, MA) and a rabbit anti-CD3 antibodies (EPITOMICS, Abcam, Cambridge, UK). After washing with PBS, sections were incubated with a goat anti-rat and goat anti-rabbit secondary antibody conjugated with AlexaFluor 488 or 594 dyes (Thermo Fisher Scientific, Waltham, MA) for 1h at room temperature.

After washing with PBS, sections were mounted with Fluoromount-G and DAPI (SouthernBiotech, Birmingham, AL), and visualized on a fluorescence microscope (Zeiss Axiophot 2, Zeiss, Oberkochen, Germany or Leica TCS-SP8 confocal microscope, Leica, Wetzlar, Germany).

VGCN , mRNA and miRNA quantification in liver and muscle tissues

Genomic DNA was extracted from frozen tissues using the MagNApure kit according to manufacturer instructions. Vector genome copy number was determined using qPCR from 20 ng of genomic DNA. A serial dilution of a DNA sample of a plasmid harboring one copy of each amplicon was used as standard curve. Real-time PCR was performed using LightCycler480 (Roche Roche, Basel, Switzerland) with 0.2 µM of each primer and 0.1 µM of the probe according to the protocol of Absolute QPCR Rox Mix (Thermo Fisher Scientific, Waltham, MA). The primer pairs and Taqman™ probes used for the human α-sarcoglycan amplification were: FWD: 5'-TGCTGGCCTATGTCATGTGC-3', REV:5'-TCTGGATGTCGGAGGTAGCC-3', and Probe: 5'-CGGGAGGGAAGGCTGAAGAGAGACC-3'. The ubiquitous acidic ribosomal phosphoprotein (P0) was used for normalization. Primer pairs and Taqman™ probe used for P0 amplification were: FWD: 5'-CTCCAAGCAGATGCAGCAGA-3', REV: 5'-ACCATGATGCGCAAGGCCAT-3' and Probe: 5'-CCGTGGTGCTGATGGGCAAGAA-3'.

mRNA and miRNA quantification

Total RNA extraction was performed from frozen tissues by Trizol™ (Thermo Fisher Scientific, Waltham, MA). Extracted RNA was dissolved in 20µl of RNase-free water and treated with Free DNA kit (Ambion) to remove residual DNA. Total RNA was quantified using a Nanodrop spectrophotometer (ND8000 Labtech, Wilmington Delaware).

Quantification of miRNAs was performed using Exiqon miRCURY LNA™ Universal RT microRNA PCR (QIAGEN, Venlo, Netherland). Total RNA (20 ng) was converted into poly-A primed universal cDNA and microRNAs were quantified in duplicate for each sample with miRNA-specific LNA primers on the LightCycler480 (Roche, Basel, Switzerland) following manufacturer's guidelines. Quantification cycle (Cq) values were calculated with the LightCycler® 480 SW 1.5.1 using 2nd Derivative Max method. RT-qPCR results, expressed as raw Cq were normalized to the miRNAs identified as the most stable, miR-16 for individual assays in serum, and miR-93 in muscle samples. The relative expression was calculated using the $2^{-\Delta Ct}$ method.

For quantification of the transgene expression, one µg of RNA was reverse-transcribed using the SuperScript II first strand synthesis kit (Thermo Fisher Scientific, Waltham, MA) and a mixture of random oligonucleotides and oligo-dT. Real-time PCR was performed using LightCycler480 (Roche, Basel, Switzerland) with 0.2 µM of each primer and 0.1 µM of the probe according to the protocol of Absolute QPCR Rox Mix (Thermo Fisher Scientific, Waltham, MA). The primer pairs and Taqman™ probes used for the human α-sarcoglycan amplification were: FWD: 5'-TGCTGGCCTATGTCATGTGC-3', REV: 5'-TCTGGATGTCGGAGGTAGCC-3', and Probe: 5'-CGGGAGGGAAGGCTGAAGAGAGACC-3'. The ubiquitous acidic ribosomal phosphoprotein (P0) was used to normalize the data across samples. The primer pairs and

Taqman™ probe used for P0 amplification were: FWD: 5'-CTCCAAGCAGATGCAGCAGA-3', REV: 5'-ACCATGATGCGCAAGGCCAT-3' and Probe: 5'-CCGTGGTGCTGATGGGCAAGAA-3'. For IFN-γ, CD-8, CD4, FOX-P3, LAG3, PD-1, PD-L1, PD-L2, TIM3, CTLA4, 2B4, commercial sets of primers and probes were used (Thermo Fisher Scientific, Waltham, MA). Each experiment was performed in duplicate.

Anti-hSGCA ELISA, ELISPOT and cytometry

Anti-hSGCA ELISA, ELISPOT and cytometry were performed as already described.[56] Briefly, blood samples were collected by retro-orbital bleeding and quickly centrifuged 10 minutes at 10000 x g. Serum samples were collected and stored at −80°C.

Recombinant hSGCA-GST (Abnova, Taipei City, Taiwan) was dissolved in carbonate buffer and coated to each well of a 96-well plate overnight at 4°C. After washing with phosphate buffered saline (PBS) containing 0.05% Tween 20 (PBS-T), three-fold serial dilutions from 1:10 to 1:21 870 of each sera were added to the plate, and incubated 2 hours at 37°C. The wells were washed with PBS-T, incubated with a 1:1000 dilution of HRP-conjugated sheep anti-mouse IgG (SouthernBiotech, Birmingham, AL) at room temperature for 1 hour, washed, and finally, added with TMB agent substrate (Sigma Aldrich, Saint-Louis, MO). After a fifteen-minute incubation, the reaction was stopped with 1N sulfuric acid solution. Absorbance values of the plates were read at 405 nm with an Enspire microplate reader. Antibody titer was determined as the last dilution that give an absorbance value above 0.5.

IFN-γ ELISPOT et IFN-γ ELISA

IFN-γ enzyme-linked immunospot (ELISPOT) assay was performed by culturing 2 x 10^5 splenocytes per well in IFN-γ Enzyme-Linked Immunospot plates (MAHAS45, Millipore, Molsheim, France). Five peptide epitopes of human alpha-sarcoglycan with the highest probability of presentation by H-2Kb MHC class I molecules were identified by Immune Epitope Database (www.iedb.org) and synthesized by GeneCust. Cells were stimulated either with one of this peptides or with 1µM hSGCA-GST recombinant protein or with SIINFEKL peptide . As a positive control, cells were stimulated with 5µg/ml of Concanavalin A (Sigma Aldrich, Saint-Louis, MO). After 24 h of culture at 37°C, plates were washed and the secretion of IFNγ was revealed with a biotinylated anti-IFNγ antibody (eBiosciences, Thermo Fisher Scientific, Waltham, MA), Streptavidin-Alkaline Phosphatase (Roche Diagnostics, Mannheim, Germany), and BCIP/NBT substrate (Mabtech, Les Ulis, France). Spots were counted using an AID reader (Cepheid Benelux, Leuven, Belgium) and the AID ELISpot Reader v6.0 software. Spot forming units (SFU) per million cells were represented after subtraction of background values obtained with unstimulated splenocytes.

IFN-γ secreted by splenocytes stimulated with the recombinant protein hSGCA-GST was measured with the Mouse IFN-gamma Quantikine ELISA Kit (R&D systems, Minneapolis, MN).

Flow cytometry analysis

Single-cell suspensions from spleen and liver were prepared and stained for surface and markers with different fluorochrome combinations: anti-CD45 (V450, clone 30-F11, BD Biosciences, San Jose, CA), anti-CD4 (V500, clone RM4-5, BD Biosciences, San Jose, CA), anti-CD8 (AF700, clone 53-6.7, BD Biosciences, San Jose, CA), anti-CD25 (PE-Cy7, clone PC-61.5, BD Biosciences, San Jose, CA), anti-PD-1 (PE-CF594, clone J43, BD Biosciences, San Jose, CA), anti-LAG-3 (PerCP-Cy5.5, clone C9B7W, BD Biosciences, San Jose, CA), anti-TIM-3 (PE-Cy7, clone C9B7W, ThermoFisher Scientific, Waltham, MA), anti-CD44

(PerCP-Cy5.5, clone IM7, ThermoFisher Scientific, Waltham, MA), iTAg^{TM} MHC Tetramer H-2 Kb OVA tetramer-SIINFEKL-PE (MBL, Woburn, MA) followed by cell viability staining using Fixable Live/Dead kit (Biolegend, San Diego, CA) according to manufacturer's instructions. Intracellular staining of FoxP3 (APC, clone FJK-16s, Thermo Fisher Scientific, Waltham, MA) was performed after fixation and permeabilization using murine FoxP3 buffer kit (Thermo Fisher Scientific, Waltham, MA) according to manufacturer's instructions. All antibodies were used at one test per 10^6 cells. Samples were acquired using Sony Spectral cell analyzer SP6800 (Sony Biotechnology Inc., San Jose, CA). Data analysis was performed using the SP6800 software (Sony Biotechnology Inc. San Jose, CA) and Kaluza software (Beckman Coulter, Indianapolis, IN).

Statistical analyses

Statistical analyses were performed using the GraphPad Prism version 6.04 (GraphPad Software, San Diego, CA). Statistical analyses were performed by ANOVA with Tukey's multiple comparison test for all the data excepted for ELISPOT and ELISA experiments where a Kruskal-Wallis with Dunn's multiple comparison test was used. In Figure 1, where we compared only Muscle vs. Muscle-Liver groups of mice, we used student t test for all the data and non-parametric Mann-Whitney for the quantification of anti-hSGCA antibodies by ELISA. Data were expressed as mean ± SD. P values of less than 0.05 were considered statistically significant.

Author contributions

G.R., I.R., F.M. and J.P. designed experiments and wrote the manuscript. G.R., J.P., H.C.V., R.H., P.C. and P.S. performed experiments. L.B. and J.D. participated in the discussion of some of the results. F.C. provided reagents. G.R. and J.P. analyzed data. G.R., F.M. and I.R. supervised the project.

Acknowledgments

This work was supported by the European Union, ERC-2013-CoG Consolidator Grant, grant agreement number 617432 (MoMAAV to F.M.), European Union's research and innovation program under Grant Agreements No. 667751 (Myocure, to F.M.) and No. 658712 (GLYCODIS3 to F.M. and G.R.), E-Rare2 grant SMART-HaemoCare (to F.M.), ANR-JCJC grant CE18-0014-01 (TRACeGSDIII, to G.R.) and the ASTRE laboratories of the Essonne general council grant (to F. M.).

Conflict of Interest Statement

All authors declare no conflicts of interest with the content of the current manuscript. F.M. is currently employee of Spark Therapeutics, Inc., a company involved in the development and commercialization of AAV gene therapies.

References

1. Nathwani, AC, Reiss, UM, Tuddenham, EG, Rosales, C, Chowdary, P, McIntosh, J*, et al.* (2014). Long-term safety and efficacy of factor IX gene therapy in hemophilia B. *N Engl J Med* **371**: 1994-2004.
2. George, LA, Sullivan, SK, Giermasz, A, Rasko, JEJ, Samelson-Jones, BJ, Ducore, J*, et al.* (2017). Hemophilia B Gene Therapy with a High-Specific-Activity Factor IX Variant. *N Engl J Med* **377**: 2215-2227.
3. Calne, R, and Davies, H (1994). Organ graft tolerance: the liver effect. *Lancet* **343**: 67-68.
4. Rehermann, B, and Nascimbeni, M (2005). Immunology of hepatitis B virus and hepatitis C virus infection. *Nat Rev Immunol* **5**: 215-229.
5. Makarova-Rusher, OV, Medina-Echeverz, J, Duffy, AG, and Greten, TF (2015). The yin and yang of evasion and immune activation in HCC. *J Hepatol* **62**: 1420-1429.
6. Dobrzynski, E, Mingozzi, F, Liu, YL, Bendo, E, Cao, O, Wang, L*, et al.* (2004). Induction of antigen-specific CD4+ T-cell anergy and deletion by in vivo viral gene transfer. *Blood* **104**: 969-977.
7. Akbarpour, M, Goudy, KS, Cantore, A, Russo, F, Sanvito, F, Naldini, L*, et al.* (2015). Insulin B chain 9-23 gene transfer to hepatocytes protects from type 1 diabetes by inducing Ag-specific FoxP3+ Tregs. *Sci Transl Med* **7**: 289ra281.
8. Dobrzynski, E, and Herzog, RW (2005). Tolerance induction by viral in vivo gene transfer. *Clin Med Res* **3**: 234-240.
9. Blackburn, SD, Shin, H, Haining, WN, Zou, T, Workman, CJ, Polley, A*, et al.* (2009). Coregulation of CD8+ T cell exhaustion by multiple inhibitory receptors during chronic viral infection. *Nature immunology* **10**: 29-37.
10. Kumar, SRP, Hoffman, BE, Terhorst, C, de Jong, YP, and Herzog, RW (2017). The Balance between CD8(+) T Cell-Mediated Clearance of AAV-Encoded Antigen in the Liver and Tolerance Is Dependent on the Vector Dose. *Mol Ther* **25**: 880-891.
11. Tay, SS, Wong, YC, McDonald, DM, Wood, NA, Roediger, B, Sierro, F*, et al.* (2014). Antigen expression level threshold tunes the fate of CD8 T cells during primary hepatic immune responses. *Proc Natl Acad Sci U S A* **111**: E2540-2549.
12. Cao, O, Dobrzynski, E, Wang, L, Nayak, S, Mingle, B, Terhorst, C*, et al.* (2007). Induction and role of regulatory CD4+CD25+ T cells in tolerance to the transgene product following hepatic in vivo gene transfer. *Blood* **110**: 1132-1140.
13. Crudele, JM, Finn, JD, Siner, JI, Martin, NB, Niemeyer, GP, Zhou, S*, et al.* (2015). AAV liver expression of FIX-Padua prevents and eradicates FIX inhibitor without increasing thrombogenicity in hemophilia B dogs and mice. *Blood* **125**: 1553-1561.
14. Herzog, RW, Mount, JD, Arruda, VR, High, KA, and Lothrop, CD, Jr. (2001). Muscle-directed gene transfer and transient immune suppression result in sustained partial correction of canine hemophilia B caused by a null mutation. *Mol Ther* **4**: 192-200.
15. Ohshima, S, Shin, JH, Yuasa, K, Nishiyama, A, Kira, J, Okada, T*, et al.* (2009). Transduction efficiency and immune response associated with the administration of AAV8 vector into dog skeletal muscle. *Mol Ther* **17**: 73-80.
16. Gao, G, Lebherz, C, Weiner, DJ, Grant, R, Calcedo, R, McCullough, B*, et al.* (2004). Erythropoietin gene therapy leads to autoimmune anemia in macaques. *Blood* **103**: 3300-3302.
17. Mendell, JR, Campbell, K, Rodino-Klapac, L, Sahenk, Z, Shilling, C, Lewis, S*, et al.* (2010). Dystrophin immunity in Duchenne's muscular dystrophy. *N Engl J Med* **363**: 1429-1437.
18. Villalta, SA, Rosenthal, W, Martinez, L, Kaur, A, Sparwasser, T, Tidball, JG*, et al.* (2014). Regulatory T cells suppress muscle inflammation and injury in muscular dystrophy. *Sci Transl Med* **6**: 258ra142.

19. Burzyn, D, Kuswanto, W, Kolodin, D, Shadrach, JL, Cerletti, M, Jang, Y*, et al.* (2013). A special population of regulatory T cells potentiates muscle repair. *Cell* **155**: 1282-1295.
20. Gross, DA, Leboeuf, M, Gjata, B, Danos, O, and Davoust, J (2003). CD4+CD25+ regulatory T cells inhibit immune-mediated transgene rejection. *Blood* **102**: 4326-4328.
21. Colella, P (2018). AAV gene transfer with tandem promoter design prevents anti-transgene immunity and provides persistent efficacy in neonate Pompe disease mice. *Mol Ther*.
22. Doerfler, PA, Todd, AG, Clement, N, Falk, DJ, Nayak, S, Herzog, RW*, et al.* (2016). Copackaged AAV9 Vectors Promote Simultaneous Immune Tolerance and Phenotypic Correction of Pompe Disease. *Hum Gene Ther* **27**: 43-59.
23. Boisgerault, F, Gross, DA, Ferrand, M, Poupiot, J, Darocha, S, Richard, I*, et al.* (2013). Prolonged gene expression in muscle is achieved without active immune tolerance using microRNA 142.3p-regulated rAAV gene transfer. *Hum Gene Ther*.
24. Dobrzynski, E, Fitzgerald, JC, Cao, O, Mingozzi, F, Wang, L, and Herzog, RW (2006). Prevention of cytotoxic T lymphocyte responses to factor IX-expressing hepatocytes by gene transfer-induced regulatory T cells. *Proc Natl Acad Sci U S A* **103**: 4592-4597.
25. Ferrand, M, Galy, A, and Boisgerault, F (2014). A dystrophic muscle broadens the contribution and activation of immune cells reacting to rAAV gene transfer. *Gene Ther* **21**: 828-839.
26. Israeli, D, Poupiot, J, Amor, F, Charton, K, Lostal, W, Jeanson-Leh, L*, et al.* (2016). Circulating miRNAs are generic and versatile therapeutic monitoring biomarkers in muscular dystrophies. *Sci Rep* **6**: 28097.
27. Xu, D, and Walker, CM (2011). Continuous CD8(+) T-cell priming by dendritic cell cross-presentation of persistent antigen following adeno-associated virus-mediated gene delivery. *J Virol* **85**: 12083-12086.
28. John, B, and Crispe, IN (2004). Passive and active mechanisms trap activated CD8+ T cells in the liver. *J Immunol* **172**: 5222-5229.
29. Sykulev, Y, Brunmark, A, Tsomides, TJ, Kageyama, S, Jackson, M, Peterson, PA*, et al.* (1994). High-affinity reactions between antigen-specific T-cell receptors and peptides associated with allogeneic and syngeneic major histocompatibility complex class I proteins. *Proc Natl Acad Sci U S A* **91**: 11487-11491.
30. Anderson, AC, Joller, N, and Kuchroo, VK (2016). Lag-3, Tim-3, and TIGIT: Co-inhibitory Receptors with Specialized Functions in Immune Regulation. *Immunity* **44**: 989-1004.
31. Boisgerault, F, and Mingozzi, F (2015). The Skeletal Muscle Environment and Its Role in Immunity and Tolerance to AAV Vector-Mediated Gene Transfer. *Current gene therapy* **15**: 381-394.
32. Cohn, EF, Zhuo, J, Kelly, ME, and Chao, HJ (2007). Efficient induction of immune tolerance to coagulation factor IX following direct intramuscular gene transfer. *J Thromb Haemost* **5**: 1227-1236.
33. Ferrer, A, Wells, KE, and Wells, DJ (2000). Immune responses to dystropin: implications for gene therapy of Duchenne muscular dystrophy. *Gene Ther* **7**: 1439-1446.
34. Flanigan, KM, Campbell, K, Viollet, L, Wang, W, Gomez, AM, Walker, CM*, et al.* (2013). Anti-dystrophin T cell responses in Duchenne muscular dystrophy: prevalence and a glucocorticoid treatment effect. *Hum Gene Ther* **24**: 797-806.
35. Le Guiner, C, Servais, L, Montus, M, Larcher, T, Fraysse, B, Moullec, S*, et al.* (2017). Long-term microdystrophin gene therapy is effective in a canine model of Duchenne muscular dystrophy. *Nature communications* **8**: 16105.
36. Haurigot, V, Mingozzi, F, Buchlis, G, Hui, DJ, Chen, Y, Basner-Tschakarjan, E*, et al.* (2010). Safety of AAV factor IX peripheral transvenular gene delivery to muscle in hemophilia B dogs. *Mol Ther* **18**: 1318-1329.
37. Ge, Y, Powell, S, Van Roey, M, and McArthur, JG (2001). Factors influencing the development of an anti-factor IX (FIX) immune response following administration of adeno-associated virus-FIX. *Blood* **97**: 3733-3737.

38. Cunningham, EC, Tay, SS, Wang, C, Rtshiladze, M, Wang, ZZ, McGuffog, C*, et al.* (2013). Gene therapy for tolerance: high-level expression of donor major histocompatibility complex in the liver overcomes naive and memory alloresponses to skin grafts. *Transplantation* **95**: 70-77.
39. Luth, S, Huber, S, Schramm, C, Buch, T, Zander, S, Stadelmann, C*, et al.* (2008). Ectopic expression of neural autoantigen in mouse liver suppresses experimental autoimmune neuroinflammation by inducing antigen-specific Tregs. *J Clin Invest* **118**: 3403-3410.
40. Lapierre, P, Janelle, V, Langlois, MP, Tarrab, E, Charpentier, T, and Lamarre, A (2015). Expression of Viral Antigen by the Liver Leads to Chronic Infection Through the Generation of Regulatory T Cells. *Cell Mol Gastroenterol Hepatol* **1**: 325-341 e321.
41. Mingozzi, F, Liu, YL, Dobrzynski, E, Kaufhold, A, Liu, JH, Wang, Y*, et al.* (2003). Induction of immune tolerance to coagulation factor IX antigen by in vivo hepatic gene transfer. *J Clin Invest* **111**: 1347-1356.
42. Follenzi, A, Battaglia, M, Lombardo, A, Annoni, A, Roncarolo, MG, and Naldini, L (2004). Targeting lentiviral vector expression to hepatocytes limits transgene-specific immune response and establishes long-term expression of human antihemophilic factor IX in mice. *Blood* **103**: 3700-3709.
43. Sun, B, Bird, A, Young, SP, Kishnani, PS, Chen, YT, and Koeberl, DD (2007). Enhanced response to enzyme replacement therapy in Pompe disease after the induction of immune tolerance. *Am J Hum Genet* **81**: 1042-1049.
44. Finn, JD, Ozelo, MC, Sabatino, DE, Franck, HW, Merricks, EP, Crudele, JM*, et al.* (2010). Eradication of neutralizing antibodies to factor VIII in canine hemophilia A after liver gene therapy. *Blood* **116**: 5842-5848.
45. Mingozzi, F, Hasbrouck, NC, Basner-Tschakarjan, E, Edmonson, SA, Hui, DJ, Sabatino, DE*, et al.* (2007). Modulation of tolerance to the transgene product in a nonhuman primate model of AAV-mediated gene transfer to liver. *Blood* **110**: 2334-2341.
46. Bartolo, L, Li Chung Tong, S, Chappert, P, Urbain, D, Collaud, F, Colella, P*, et al.* (2019). Dual muscle-liver transduction imposes immune tolerance for muscle transgene engraftment despite preexisting immunity. *JCI Insight* **4**.
47. Markusic, DM, Hoffman, BE, Perrin, GQ, Nayak, S, Wang, X, LoDuca, PA*, et al.* (2013). Effective gene therapy for haemophilic mice with pathogenic factor IX antibodies. *EMBO Mol Med* **5**: 1698-1709.
48. Han, SO, Ronzitti, G, Arnson, B, Leborgne, C, Li, S, Mingozzi, F*, et al.* (2017). Low-Dose Liver-Targeted Gene Therapy for Pompe Disease Enhances Therapeutic Efficacy of ERT via Immune Tolerance Induction. *Mol Ther Methods Clin Dev* **4**: 126-136.
49. Paul-Heng, M, Leong, M, Cunningham, E, Bunker, DLJ, Bremner, K, Wang, Z*, et al.* (2018). Direct recognition of hepatocyte-expressed MHC class I alloantigens is required for tolerance induction. *JCI Insight* **3**.
50. Lichtenegger, FS, Rothe, M, Schnorfeil, FM, Deiser, K, Krupka, C, Augsberger, C*, et al.* (2018). Targeting LAG-3 and PD-1 to Enhance T Cell Activation by Antigen-Presenting Cells. *Front Immunol* **9**: 385.
51. Stross, L, Gunther, J, Gasteiger, G, Asen, T, Graf, S, Aichler, M*, et al.* (2012). Foxp3+ regulatory T cells protect the liver from immune damage and compromise virus control during acute experimental hepatitis B virus infection in mice. *Hepatology (Baltimore, Md)* **56**: 873-883.
52. Grinberg-Bleyer, Y, Saadoun, D, Baeyens, A, Billiard, F, Goldstein, JD, Gregoire, S*, et al.* (2010). Pathogenic T cells have a paradoxical protective effect in murine autoimmune diabetes by boosting Tregs. *J Clin Invest* **120**: 4558-4568.
53. Ronzitti, G, Bortolussi, G, van Dijk, R, Collaud, F, Charles, S, Leborgne, C*, et al.* (2016). A translationally optimized AAV-UGT1A1 vector drives safe and long-lasting correction of Crigler-Najjar syndrome. *Mol Ther Methods Clin Dev* **3**: 16049.
54. Wang, Z, Zhu, T, Qiao, C, Zhou, L, Wang, B, Zhang, J*, et al.* (2005). Adeno-associated virus serotype 8 efficiently delivers genes to muscle and heart. *Nature biotechnology* **23**: 321-328.

55. Vandendriessche, T, Thorrez, L, Acosta-Sanchez, A, Petrus, I, Wang, L, Ma, L*, et al.* (2007). Efficacy and safety of adeno-associated viral vectors based on serotype 8 and 9 vs. lentiviral vectors for hemophilia B gene therapy. *J Thromb Haemost* **5**: 16-24.
56. Meliani, A, Boisgerault, F, Hardet, R, Marmier, S, Collaud, F, Ronzitti, G*, et al.* (2018). Antigen-selective modulation of AAV immunogenicity with tolerogenic rapamycin nanoparticles enables successful vector re-administration. *Nature communications* **9**: 4098.

Figure legends

Figure 1. Simultaneous liver and muscle targeting improves transgene expression in dystrophic muscle. (A) Five week-old Sgca$^{-/-}$ mice were intramuscularly injected (IM, *Tibialis Anterior,* TA) at day 0 (D0) with 5 x10^{9} vg/mouse of AAV6-SPc5.12-hSGCA vector. Five days after IM injection (D5) mice received an intravenous injection (IV) with either 5 x10^{11} vg/mouse of AAV9-hAAT-hSGCA (Muscle-Liver) or an empty AAV9 vector (Muscle). In parallel, a group of mice injected intramuscularly with PBS and intravenously with the empty AAV9 vector was used as control (Control). Two months after treatment, mice were sacrificed and tissues collected. **(B)** Hematoxylin phloxine saffron staining (HPS, upper panel, scale bar = 100µm) performed in TA. **(C)** Immunostaining anti-hSGCA (green), CD8 (red) and DAPI (blue) performed in TA**.** White arrows indicate CD8 cells. Scale bar = 50µm. **(D)** miR-206 levels measured in TA and represented as fold-change versus wild type C57BL/6J mice (dotted line in the graph). **(E)** Vector genome copy number (VGCN) per diploid genome measured in TA. **(F)** Anti-hSGCA IgG titers measured by ELISA using recombinant hSGCA protein. **(G, H)** CD8 and IFNγ mRNA measured in TA. **(I)** IFNγ secretion from recombinant hSGCA-stimulated splenocytes measured by ELISA. Data were expressed as mean ± SD. Statistical analyses were performed by student t test in panel D, E, G, H and I; a non-parametric Mann-Whitney test was used for panel F (* = $p<0.05$, † = $p<0.05$ as indicated, n=2 for Control, n=4 for Muscle and n=6 for Muscle-Liver).

Figure 2. Liver transduction controls preexisting anti-hSGCA immune response in C57BL/6J mice. (A) Eight week-old C57BL/6J mice received at day 0 an intramuscular injection (IM, *Tibialis Anterior,* TA) of 2.5 x10^9 vg/mouse of AAV6-SPc5.12-hSGCA vector and at day 0 or day 15 an intravenous injection (IV) of 1 x 10^{11} vg/mouse of AAV9-hAAT-hSGCA (Muscle-Liver D0 and Muscle-Liver D15 respectively). In parallel, two groups of mice injected intramuscularly at day 0 with PBS or 2.5 x 10^9 vg/mouse of AAV6-SPc5.12-hSGCA vector were used as controls (Control and Muscle groups respectively). One month after treatment, mice were sacrificed and tissues collected. **(B)** Hematoxylin phloxine saffron staining (HPS, upper panel, scale bar = 100µm) and anti-hSGCA (green), CD8 (red) and DAPI (blue) immunostaining (lower panel, scale bar = 50µm) performed on TA muscle. White arrows indicate CD8 cells. **(C, D)** CD8 and IFNγ mRNA measured in TA. **(E)** Vector genome copy number (VGCN) per diploid genome measured in TA. Data were expressed as mean ± SD. Statistical analyses were performed by ANOVA (* = $p<0.05$, n=4 per group).

Figure 3. hSGCA-SIIN fusion transgene as a model antigen to evaluate cytotoxic response in C57BL/6J mice. **(A)** Schematic representation of the fusion between hSGCA and SIINFEKL epitope. The SIINFEKL peptide and its scrambled version FILKSINE were fused to the C-terminal domain of hSGCA (hSGCA-SIIN and hSGCA-FILK, respectively). RWLRYTQR peptide located in the extracellular domain was top-score predicted for binding on murine H-2Kb class I MHC. **(B)** Five-week old C57BL/6J mice were intramuscularly injected (IM, *Tibialis Anterior,* TA) with 1 x 10^{10} vg/mouse of AAV1 or AAV6 expressing hSGCA under the SPc5.12-promoter (AAV1-hSGCA, AAV6-hSGCA) or with the same dose of an AAV1 vector expressing either the hSGCA-SIIN fusion protein (AAV1-hSGCA-SIIN) or the hSGCA-FILK fusion protein (AAV1-hSGCA-FILK) under the control of the same promoter. In parallel, one group of mice was injected intramuscularly with PBS as control (Control). Fifteen days after treatment, mice were sacrificed and tissues collected. **(C-E)** IFNγ-ELISPOT performed on splenocytes stimulated with SIINFEKL peptide **(C)**, hSGCA recombinant protein **(D)** or the RWLRYTQR peptide **(E)** derived from hSGCA. **(F)** Hematoxylin-phloxine-saffron staining (HPS, upper panel, scale bar = 100µm) and anti-hSGCA (green), CD8 (red) and DAPI (blue) immunostaining (lower panel, scale bar = 50µm) performed on TA muscle. **(G-I)** CD8, IFNγ and hSGCA mRNA measured in TA. Data were expressed as mean ± SD. Statistical analyses were performed by ANOVA in all panels except for panels C-E where a Kruskal-Wallis test was used (* = $p<0.05$, as indicated, n=4 per group).

Figure 4. Simultaneous liver and muscle expression of hSGCA-SIINFEKL controls anti-transgene immune response (A) Five-week old C57BL/6J mice intramuscularly injected (IM, *Tibialis Anterior,* TA) with 1 x 10^{10} vg/mouse of AAV1-SPc5.12-hSGCA-SIINFEKL vector and intravenously injected with 1 x 10^{11} vg/mouse of AAV9-hAAT-hSGCA-SIINFEKL (Muscle-Liver). Two groups of mice received the two vectors separately either by intramuscular (Muscle) or intravenous (Liver) injection. PBS-injected mice were used as controls (Control). One month after treatment, mice were sacrificed and tissues collected. **(B)** IFNγ-ELISPOT performed on splenocytes stimulated with SIINFEKL peptide. **(C)** Anti-hSGCA IgG titers measured by ELISA using recombinant hSGCA protein. **(D)** Vector genome copy number (VGCN) per diploid genome measured in TA. **(E, F)** CD8 and IFNγ mRNA measured in TA. **(G)** anti-hSGCA (green), CD8 (red) and DAPI (blue) immunostaining performed in TA muscle (scale bar = 50 µm). White arrows indicate CD8 positive cells. **(H)** Vector genome copy number (VGCN) per diploid genome measured in liver. **(I, L)** CD8 and IFNγ mRNA measured in liver. Data were expressed as mean ± SD. Statistical analyses were performed by ANOVA in all panels except for panel B and C where a Kruskal-Wallis test was used (* = $p<0.05$, as indicated, n=3 per group).

Figure 5. Simultaneous liver and muscle expression of hSGCA-SIINFEKL increases liver intraparenchymal T-regulatory cells and exhausted CD8 T-cells. Non-parenchymal cells extracted from livers of mice treated as described in figure 4 were analyzed by flow cytometry. **(A, B)** Flow cytometry histograms representing the CD4+ Foxp3+ population gated on CD4+ cells. The histogram shows quantification. **(C, D)** Flow cytometry dot plots representing the CD8+ PD1+ population gated on CD8+ cells. The histogram shows the quantification of the dot plots. **(E, F)** Flow cytometry dot plots representing the CD8+ PD1+ LAG3+ population gated on CD8+ cells. The histogram shows the quantification of the dot plots. **(G, H)** Flow cytometry dot plots representing the CD8+ PD1+ TIM3+ population gated on CD8+ cells. The histogram shows the quantification of the dot plots. In C,E,G the blue dots represent SIINFEKL-specific MHC class I dextramer stained T cells. Data were expressed as mean ± SD. Statistical analyses were performed by ANOVA (* = $p<0.05$ vs. Control, n=3 per group).

Figure 6. Immune checkpoint blockade induces liver intra-parenchymal Tregs. (A) Five-week old C57BL/6J mice were intramuscularly injected (IM, *Tibialis Anterior,* TA) with 1 x 10^{10} vg/mouse of AAV1-SPc5.12-hSGCA-SIINFEKL vector and intravenously injected with 1 x 10^{11} vg/mouse of AAV9-hAAT-hSGCA-SIINFEKL (Muscle-Liver). A group of mice treated with the same combination of vectors was treated every three days from day 2 to day 14 with the combination anti-PD1, anti-PD-L1 and anti-Lag3 antibodies (Muscle-Liver +Ab). Another group of mice received only the AAV1 vector intramuscularly (Muscle). PBS-injected mice were used as controls (Control). Two weeks after treatment, mice were sacrificed and tissues collected. **(B)** IFNγ-ELISPOT performed on splenocytes stimulated with SIINFEKL peptide. **(C)** Immunostaining anti-hSGCA (green), CD8 (red) and DAPI (blue) in TA muscle (scale bar = 50µm). White arrow indicates CD8 cell. **(D)** Immunostaining anti-hSGCA (green), CD8 (red) and DAPI (blue) performed on liver (scale bar = 50µm). White arrow indicates CD8 cell. **(E)** Immunostaining anti-CD3 (green), anti-FoxP3 (Red) and DAPI (Blue) (scale bar = 25µm). White arrow indicates FoxP3 cell. **(F,G)** Flow cytometry dot plots representing the liver non-parenchymal CD4+ FoxP3+ population gated on CD4+ cells. The histogram shows the quantification of the dot plots. Data were expressed as mean ± SD. Statistical analyses were performed by ANOVA except for panel B where a Kruskal-Wallis test was used (* = $p<0.05$ vs. all groups, n=4 per group).

Figure 7. Simultaneous checkpoint blockade and Treg depletion breaks liver induced anti-transgene tolerance. (A, B) Five-week old C57BL/6J mice were intramuscularly injected (IM, *Tibialis Anterior,* TA) with 1 x 10^{10} vg/mouse of AAV1-SPc5.12-hSGCA-SIINFEKL vector and intravenously injected with PBS (Muscle) or 1 x 10^{11} vg/mouse of AAV9-hAAT-hSGCA-SIINFEKL (Muscle-Liver). A group of mice treated with the combination of vectors received a simultaneous injection of NAD and anti-CD25 at day 3 and anti-CD25 alone at day 6 and 7 (Muscle-Liver –Treg). Finally, another group of mice received the same treatment combined with the injection of anti-PD1, anti-PD-L1 and anti-LAG3 antibodies every three days from day 3 to day 12 (Muscle-Liver –Treg + Ab). Two weeks after treatment, mice were sacrificed and tissues collected. **(C)** IFNγ-ELISPOT performed on splenocytes stimulated with SIINFEKL peptide. **(D)** Liver intraparenchymal CD8+ cells gated on CD45+ cells. **(E)** Liver intraparenchymal CD8+CD44+Dextramer+ cells gated on CD8+ cells. **(F)** Vector genome copy number (VGCN) per diploid genome measured in TA. **(G)** Immunostaining anti-hSGCA (green), CD8 (red) and DAPI (blue) in TA. White arrow indicates CD8 cell. Data were expressed as mean ± SD. Statistical analyses were performed by ANOVA except for panel B where a Kruskal-Wallis test was used (* = $p<0.05$, n=4 per group).

Figure 1

a

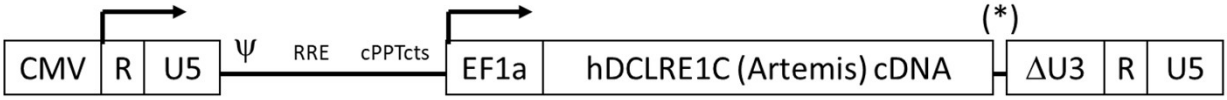
CMV
R
U5
Ψ
RRE
cPPTcts
EF1a
hDCLRE1C (Artemis) cDNA
(*)
ΔU3
R
U5

b

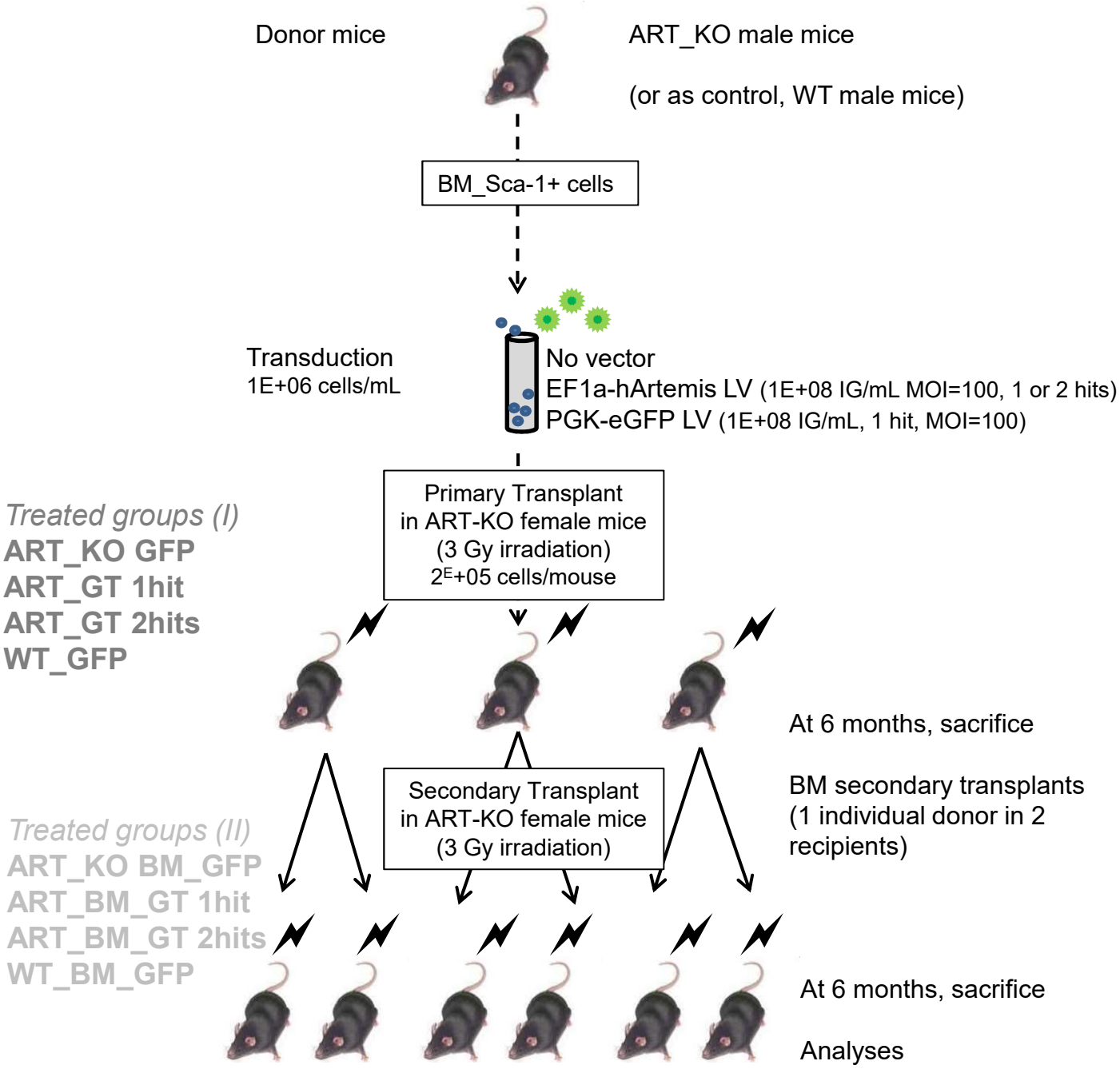
Donor mice
ART_KO male mice
(or as control, WT male mice)
BM_Sca-1+ cells
Transduction
1E+06 cells/mL
No vector
EF1a-hArtemis LV (1E+08 IG/mL MOI=100, 1 or 2 hits)
PGK-eGFP LV (1E+08 IG/mL, 1 hit, MOI=100)
Primary Transplant
in ART-KO female mice
(3 Gy irradiation)
2E+05 cells/mouse
Treated groups (I)
ART_KO GFP
ART_GT 1hit
ART_GT 2hits
WT_GFP
At 6 months, sacrifice
BM secondary transplants
(1 individual donor in 2 recipients)
Secondary Transplant
in ART-KO female mice
(3 Gy irradiation)
Treated groups (II)
ART_KO BM_GFP
ART_BM_GT 1hit
ART_BM_GT 2hits
WT_BM_GFP
At 6 months, sacrifice
Analyses

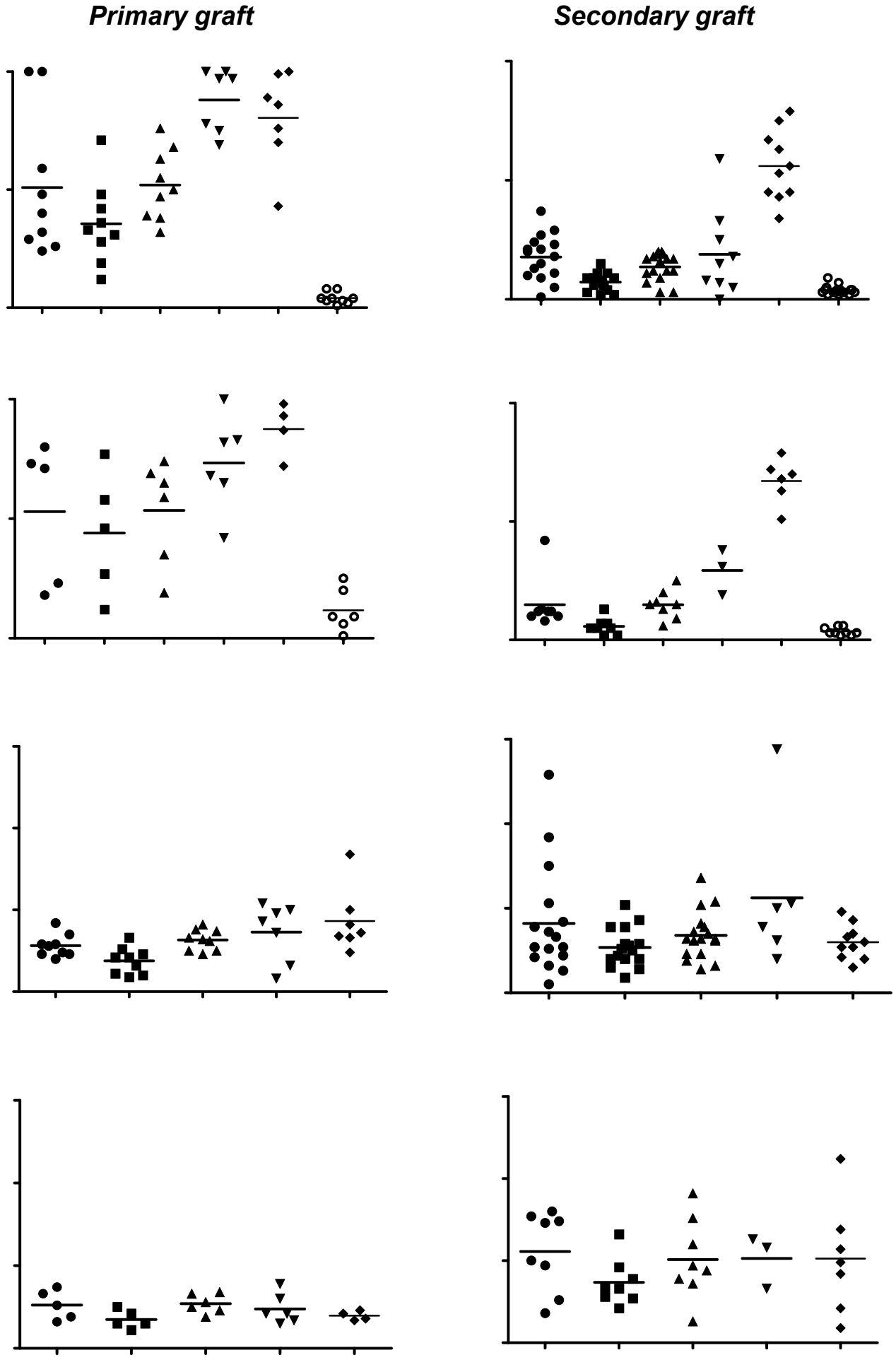
Primary graft
Secondary graft

Figure 3

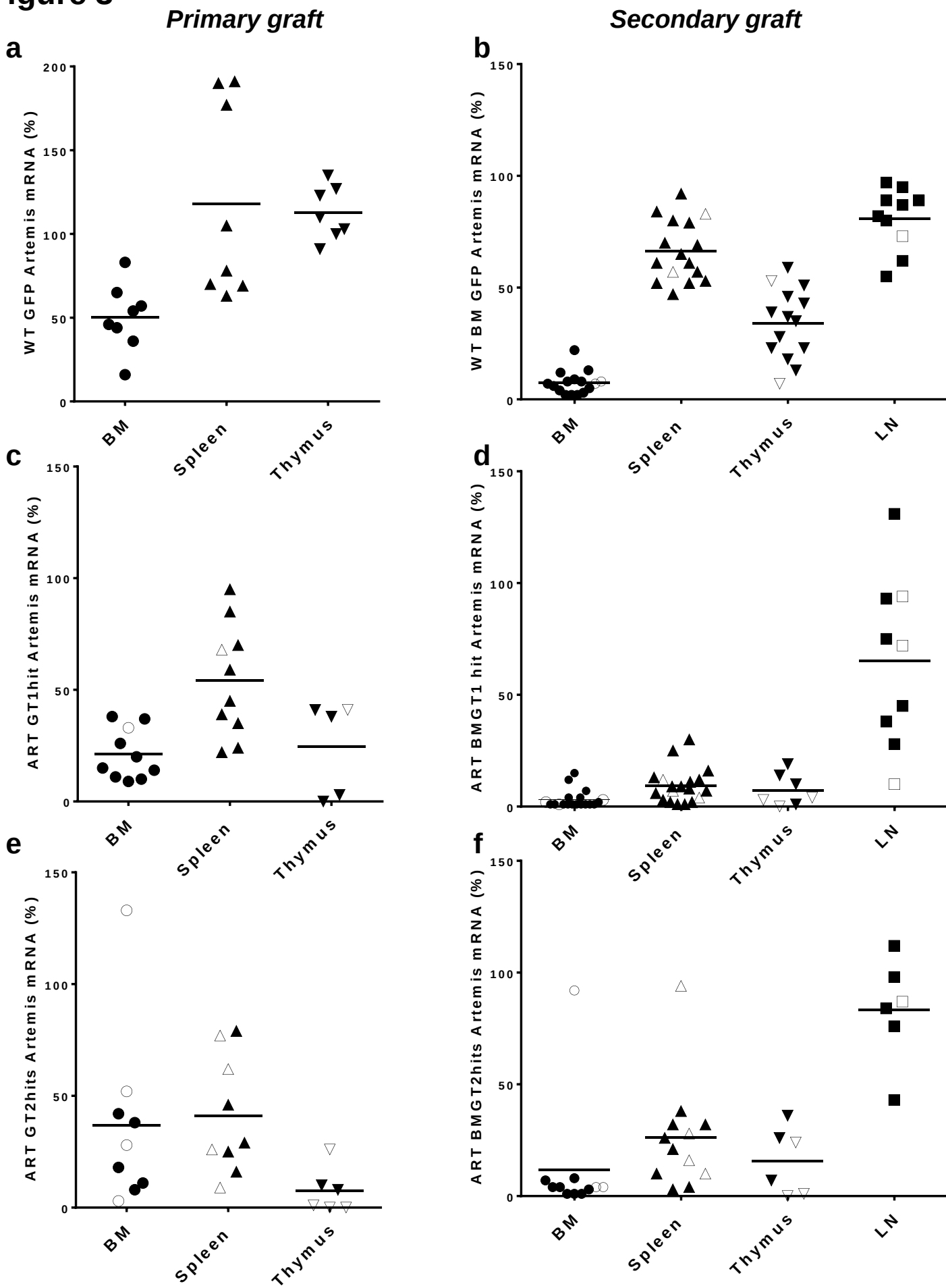
Primary graft
Secondary graft
a
b
c
d
e
f
WT GFP Artemis mRNA (%)
WT BM GFP Artemis mRNA (%)
ART GT1hit Artemis mRNA (%)
ART BMGT1 hit Artemis mRNA (%)
ART GT2hits Artemis mRNA (%)
ART BMGT2hits Artemis mRNA (%)
BM
Spleen
Thymus
LN

Figure 4

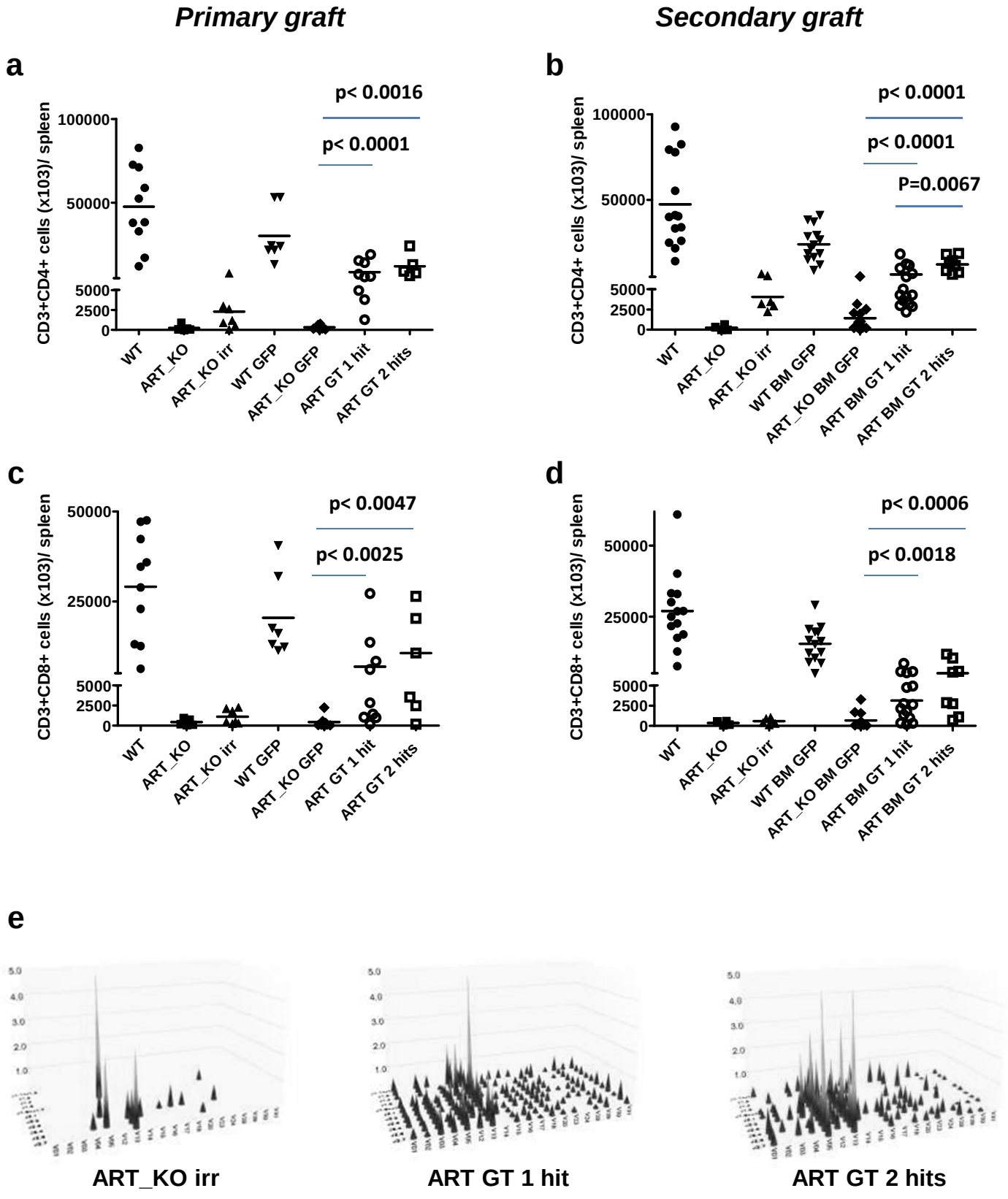
Primary graft
Secondary graft
a
b
c
d
e
CD3+CD4+ cells (x103)/ spleen
CD3+CD8+ cells (x103)/ spleen
p< 0.0016
p< 0.0001
p< 0.0001
p< 0.0001
P=0.0067
p< 0.0047
p< 0.0025
p< 0.0006
p< 0.0018
100000
50000
25000
5000
2500
0
WT
ART_KO
ART_KO irr
WT GFP
ART_KO GFP
ART GT 1 hit
ART GT 2 hits
WT BM GFP
ART_KO BM GFP
ART BM GT 1 hit
ART BM GT 2 hits
ART_KO irr
ART GT 1 hit
ART GT 2 hits

Figure 5

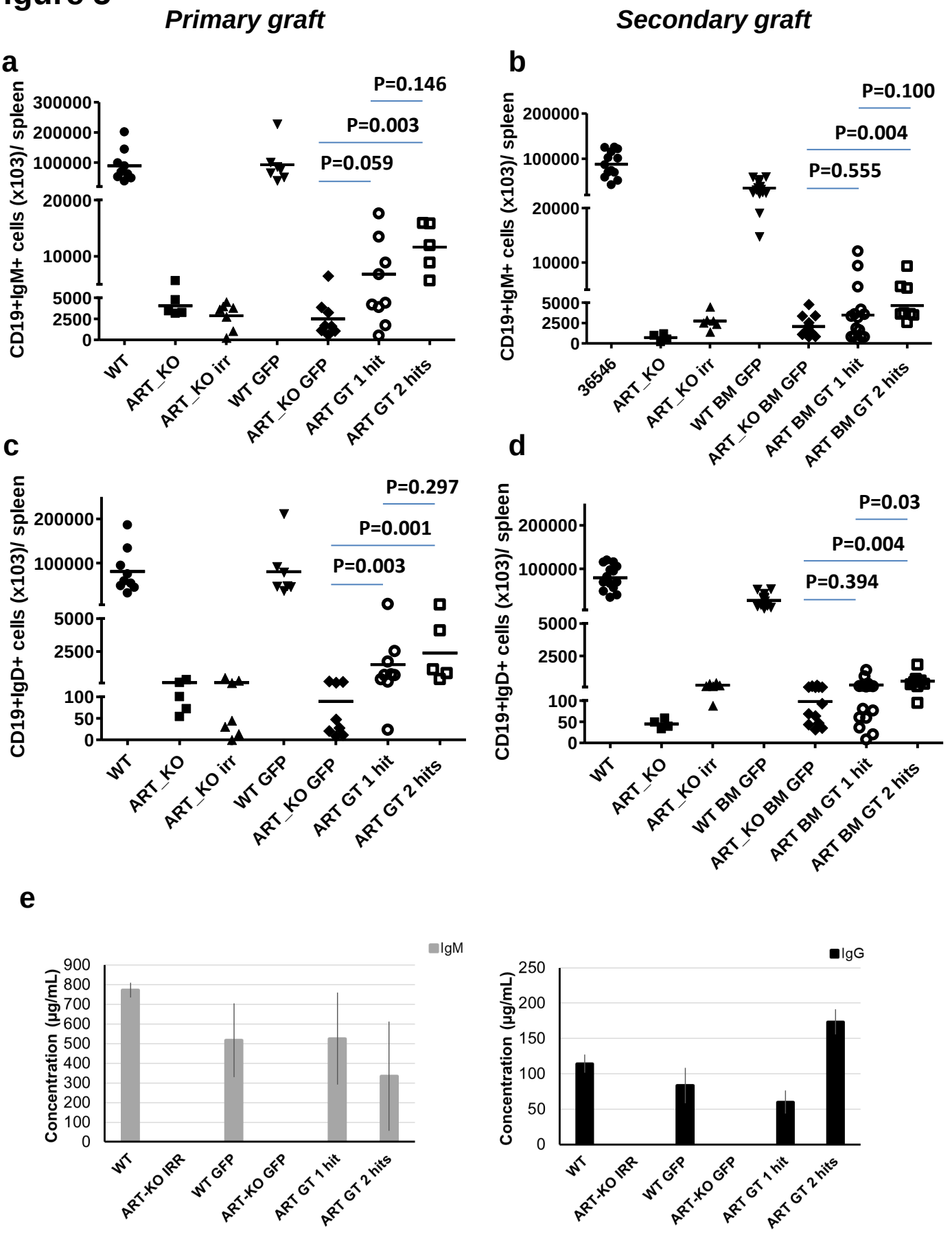
Primary graft
Secondary graft
a
CD19+IgM+ cells (x103)/ spleen
300000
200000
100000
20000
10000
5000
2500
0
P=0.146
P=0.003
P=0.059
WT
ART_KO
ART_KO irr
WT GFP
ART_KO GFP
ART GT 1 hit
ART GT 2 hits
b
CD19+IgM+ cells (x103)/ spleen
200000
100000
20000
10000
5000
2500
0
P=0.100
P=0.004
P=0.555
36546
ART_KO
ART_KO irr
WT BM GFP
ART_KO BM GFP
ART BM GT 1 hit
ART BM GT 2 hits
c
CD19+IgD+ cells (x103)/ spleen
200000
100000
5000
2500
100
50
0
P=0.297
P=0.001
P=0.003
WT
ART_KO
ART_KO irr
WT GFP
ART_KO GFP
ART GT 1 hit
ART GT 2 hits
d
CD19+IgD+ cells (x103)/ spleen
200000
100000
5000
2500
100
50
0
P=0.03
P=0.004
P=0.394
WT
ART_KO
ART_KO irr
WT BM GFP
ART_KO BM GFP
ART BM GT 1 hit
ART BM GT 2 hits
e
IgM
Concentration (µg/mL)
900
800
700
600
500
400
300
200
100
0
WT
ART-KO IRR
WT GFP
ART-KO GFP
ART GT 1 hit
ART GT 2 hits
IgG
Concentration (µg/mL)
250
200
150
100
50
0
WT
ART-KO IRR
WT GFP
ART-KO GFP
ART GT 1 hit
ART GT 2 hits

Fig re

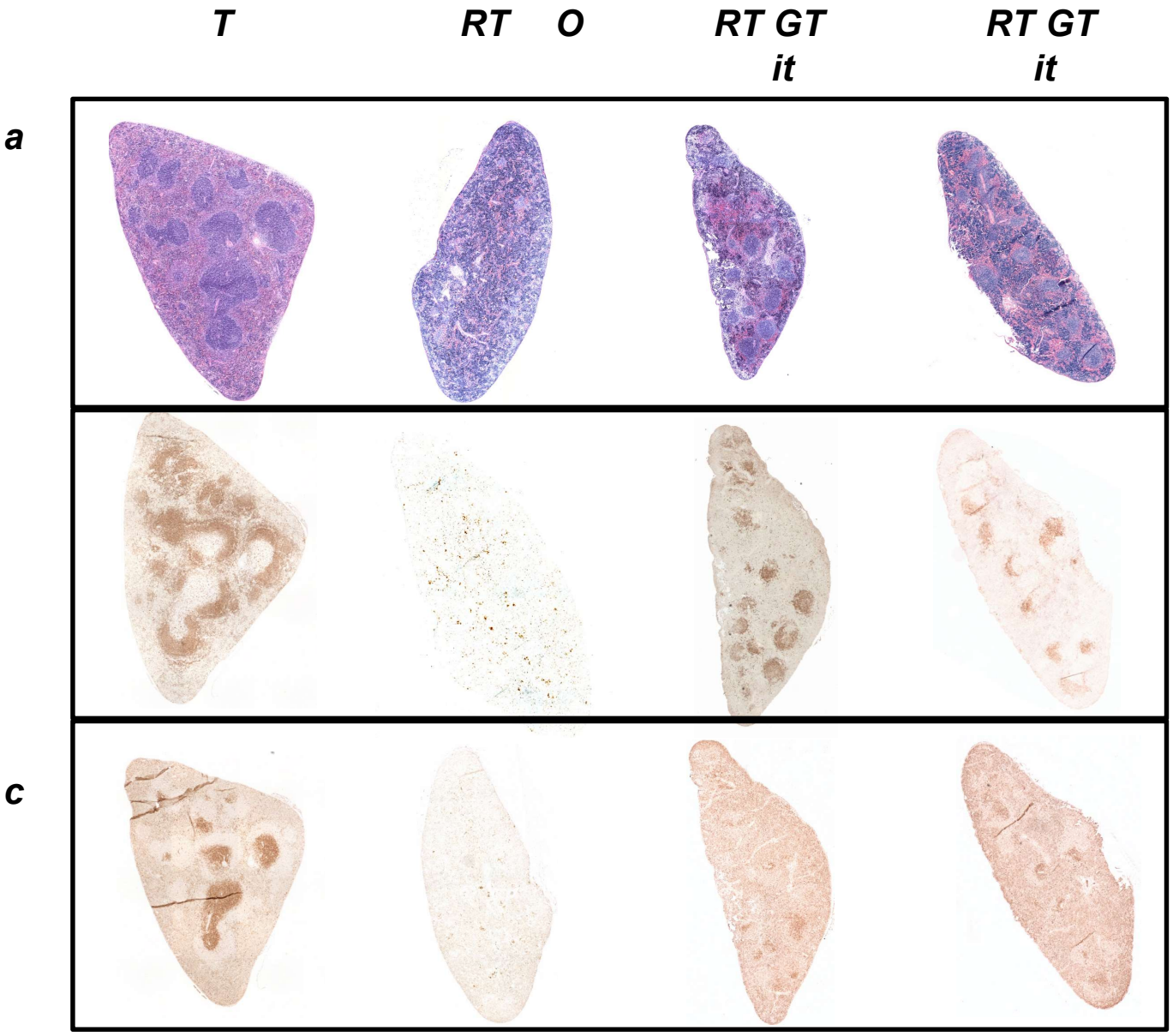

Fig re

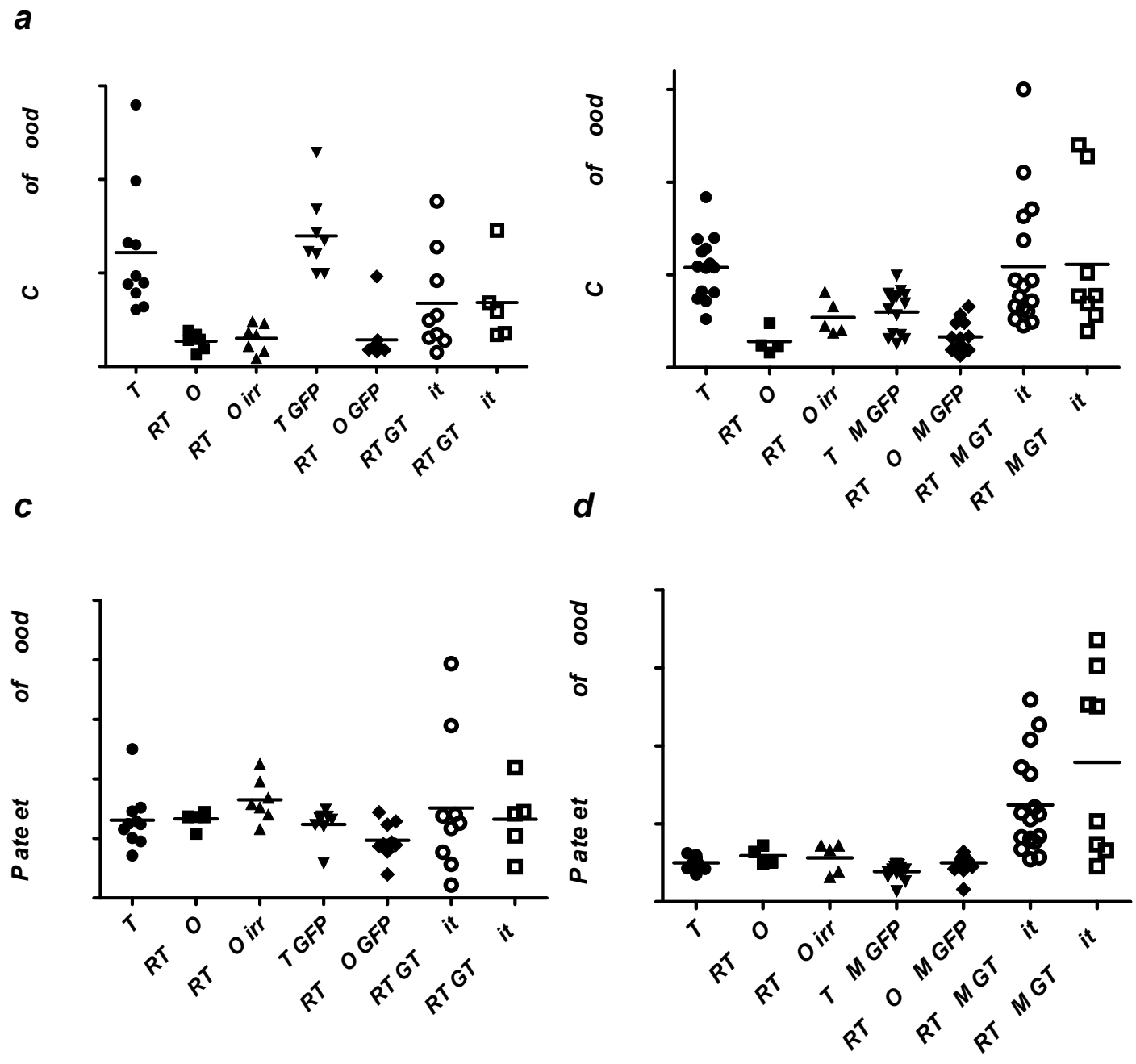
a
c of ood
T
RT O
RT O irr
T GFP
RT O GFP
RT GT it
RT GT it
c of ood
T
RT O
RT O irr
T M GFP
RT O M GFP
RT M GT it
RT M GT it
c
P ate et of ood
T
RT O
RT O irr
T GFP
RT O GFP
RT GT it
RT GT it
d
P ate et of ood
T
RT O
RT O irr
T M GFP
RT O M GFP
RT M GT it
RT M GT it

Fig re

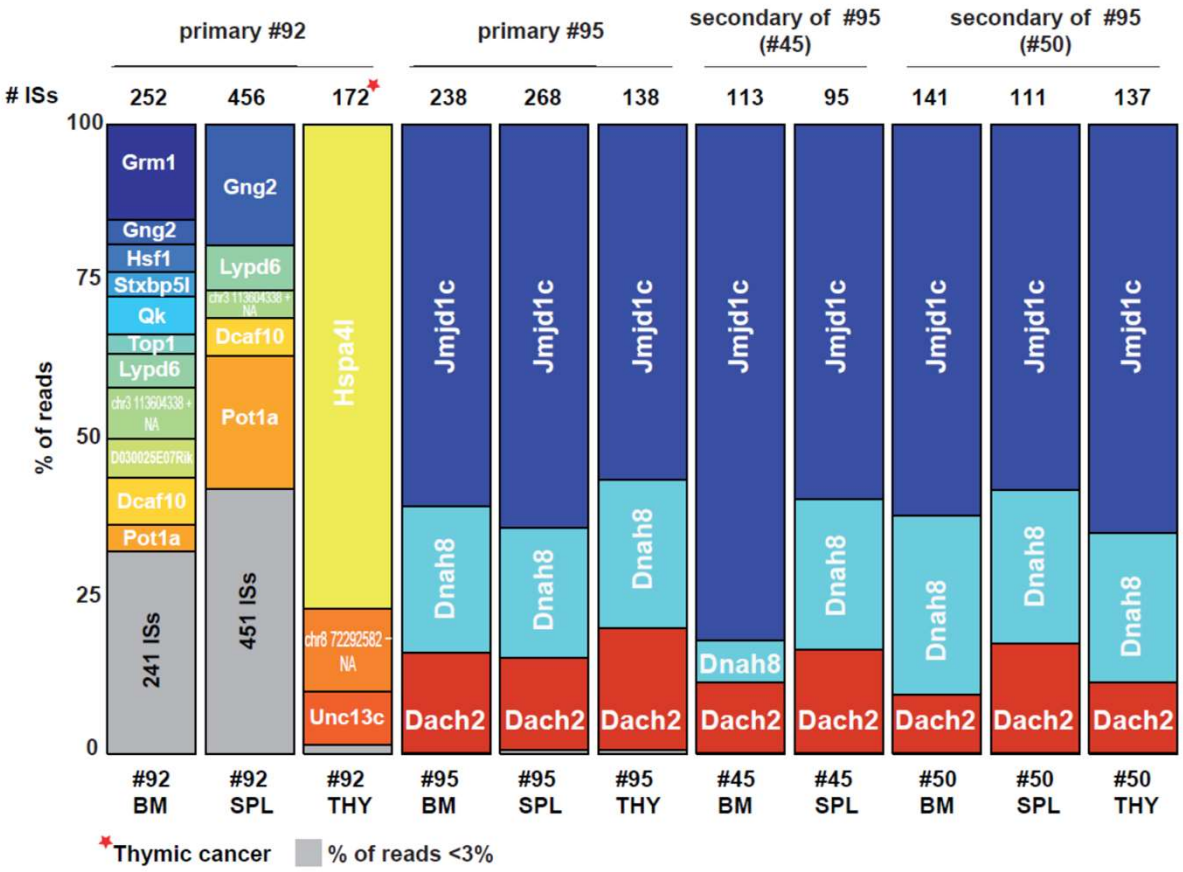
primary #92
primary #95
secondary of #95 (#45)
secondary of #95 (#50)
ISs
252
456
172
238
268
138
113
95
141
111
137
% of reads
100
75
50
25
0
Grm1
Gng2
Hsf1
Stxbp5l
Qk
Top1
Lypd6
chr3 113604338 + NA
D030025E07Rik
Dcaf10
Pot1a
241 ISs
Gng2
Lypd6
chr3 113604338 + NA
Dcaf10
Pot1a
451 ISs
Hspa4l
chr8 72292582 - NA
Unc13c
Jmjd1c
Dnah8
Dach2
#92 BM
#92 SPL
#92 THY
#95 BM
#95 SPL
#95 THY
#45 BM
#45 SPL
#50 BM
#50 SPL
#50 THY
Thymic cancer
% of reads <3%

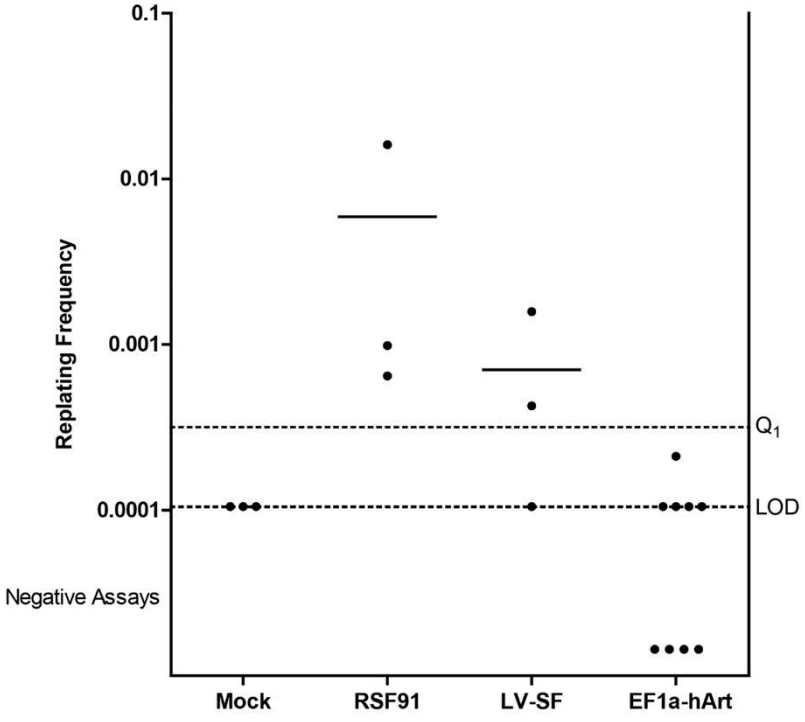
0.1
0.01
0.001
0.0001
Replating Frequency
Q1
LOD
Negative Assays
Mock
RSF91
LV-SF
EF1a-hArt